



Groundwater quality assessment using water quality index and multivariate statistical analysis case study: East Matrouh, Northwestern coast, Egypt

Rasha A. El-Kholy¹ · Ehab Zaghlool¹ · Heba Isawi¹ · Elsayed A. Soliman² · Mostafa M. H. Khalil² · Abdel-hameed M. El-Aassar¹ · Moustafa M. Said¹

Received: 1 October 2021 / Accepted: 13 March 2022 / Published online: 30 April 2022
© The Author(s), under exclusive licence to Springer-Verlag GmbH Germany, part of Springer Nature 2022

Abstract

Rapid urbanisation has had a significant negative influence on the water bodies that flow through and around urban areas. This study aims to evaluate the water quality and analyse the suitability for drinking and irrigation uses. This study envisaged assessing the water quality status of the groundwater using the pollution index of groundwater (PIG), ecological risk index (ERI) and multivariate statistical techniques, namely cluster analysis (CA) and principal component analysis (PCA), that were applied to differentiate the sources of water quality variation and determine the cause of pollution in the study area. Most groundwater is unsuitable for drinking and irrigation consumption, depending on analyses. PIG values indicated high pollution levels in the studied water body, rendering it unsuitable for any practical purpose. CA results showed the impact of surface water and treatment plant on groundwater. PCA was used to identify four important factors in the groundwater, including mineral and nutrient pollution, heavy metal pollution, organic pollution and faecal contamination. The deteriorating water quality of the groundwater was demonstrated to originate from vast sources of anthropogenic activities, especially municipal sewage discharge. Study wells had greater concentrations of Cl^- and Na^+ in their water because seawater flows into the aquifer system and mixes with the marine aquifer matrix. Thus, the current work reveals how to employ the PIG and multivariate statistical approaches to obtain more accessible and more meaningful information about the water quality of groundwater and to identify the sources of pollution.

Keywords Hydrochemical characteristics · Pollution index of groundwater · Multivariate statistical analysis

Introduction

Water security is a huge challenge for the global society's long-term prosperity. As a result of inaccurate water resource management due to environmental pressures, developing countries are today challenged with large population growth, rapid urbanisation and insufficient water-sector services (Yousif 2015). The north-west coast of Egypt is more sensitive to future sustainable development and this,

on the other hand, depends primarily on the occurrence and maintenance of water resources (Ali et al. 2007). Due to the climate change, there have been insufficient precipitation on the north-western coast of Egypt for agricultural activity and residents have started drilling water wells (Solomon et al. 2007). In such instances, groundwater is the only source of good quality freshwater, and it is widely used for residential, agricultural and industrial purposes. Due to population increase and rapid development, several places have suffered over-exploitation and uncontrolled usage of groundwater resources (Adimalla and Wu 2019). As a result, the availability of fresh groundwater has decreased, and the quality of groundwater in some locations has deteriorated. The majority of surface water is found in streams, rivers, springs, ponds, lakes and reservoirs. Surface water is gathered from rain in watershed areas, flows through streams and rivers, and settles in ponds and lakes on occasion (Manahan 2010). In the study area, surface waters are relatively inadequate,

Responsible Editor: Xianliang Yi

✉ Rasha A. El-Kholy
rasha_ali@drc.gov.eg

¹ Hydrogeochemistry Department, Desert Research Center, Cairo, Egypt

² Chemistry Department, Faculty of Science, Ain Shams University, Cairo, Egypt

uniformly scattered or unsuited to human consumption in many coastal locations (Yidana and Yidana 2010). Further research have found that direct dumping into the surviving surface water bodies of various polluted materials from home, farming and industrial wastewater eventually pollutes them (Edokpayi et al. 2017). Surface water also faces serious exposures to salinity due to sea backwater in coastal zones (Vijay et al. 2011). The surface water is quite limited in the coastal zone because of the winter precipitations (El Bastawesy et al. 2008). Agricultural production may have several factors; however, water is the most important factor (Oweis and Hachum 2003). Naturally, water can convey various heavy metals across diverse geological formations (Mohankumar et al. 2016). Biological activity, soil leaching, weathering, and rock disintegration are many instances of natural processes that produce changes in the quality of groundwater (Rao et al. 2020). Appreciation of the water body's hydrochemistry exposes water to a variety of uses (Alexakis 2011; Gamvroula et al. 2013). Groundwater quality is critical in assessing its suitability for various uses. A variety of geochemical processes, including natural and anthropogenic activities, can have an impact on the quality of groundwater. Weathering and dissolving of rocks, leaching from the soil and biological activities are all natural processes that cause variations in groundwater quality (Khatri and Tyagi 2015; Rao et al. 2020). In addition, the interaction of contaminated surface water with groundwater could threaten groundwater resources (Brindha et al. 2014). In the research field, groundwater quality may be impacted by the construction of a sewage treatment plant with a capacity of 25,000 m³/day at a height of around 60 m above sea level. The pollution index of groundwater (PIG) aims to investigate and understand the status of water quality in a water body (Horton 1965; Brown et al. 1970). The multivariate

statistical tools enable to manage water resources consistently (Bora and Goswami 2017). It aims to provide the water quality of a body a single value, which can help understand the quality of the water for various purposes (Smita et al. 2018). Other approaches, such as cluster analysis (CA) and factorial analysis (FA), help to assess the spatial and temporal variants of water quality to identify potential factors affecting water quality (Gamble and Babbar-Sebens 2012). The current investigation was shown with the following objectives: (1) make an evaluation of groundwater and surface water; (2) estimate their drinking and irrigation appropriateness; (3) identify the state of aquifers for intrusion/freshening phases that occurs over time via using the hydrochemical facies evolution.

The study area

The study area is about 10 km away from Matrouh city. It is constrained by longitudes of 27°15' and 27°25' E, latitudes of 31°8' and 31°25' N with a total area of approximately 400 km².

Three drainage basins were chosen for the present study; these basins from the northwest to the southeast are Wadi Samla, Wadi Khair and Wadi Naghamsh with an area of 26, 36 and 116 km², respectively (Fig. 1a). The chosen basins are important because of their agricultural operations, which require more water supplies to be sustainable and not transitory. The sewage treatment plant in the study area is at an altitude of approximately 60 m from sea level with a capacity of 25,000 m³/day. The plant has 14 oxidation basins used in aerobic and anaerobic treatment. The wastewater is treated and directed to three untreated dirt reservoirs used for water storage and tree forest irrigation. The wastewater

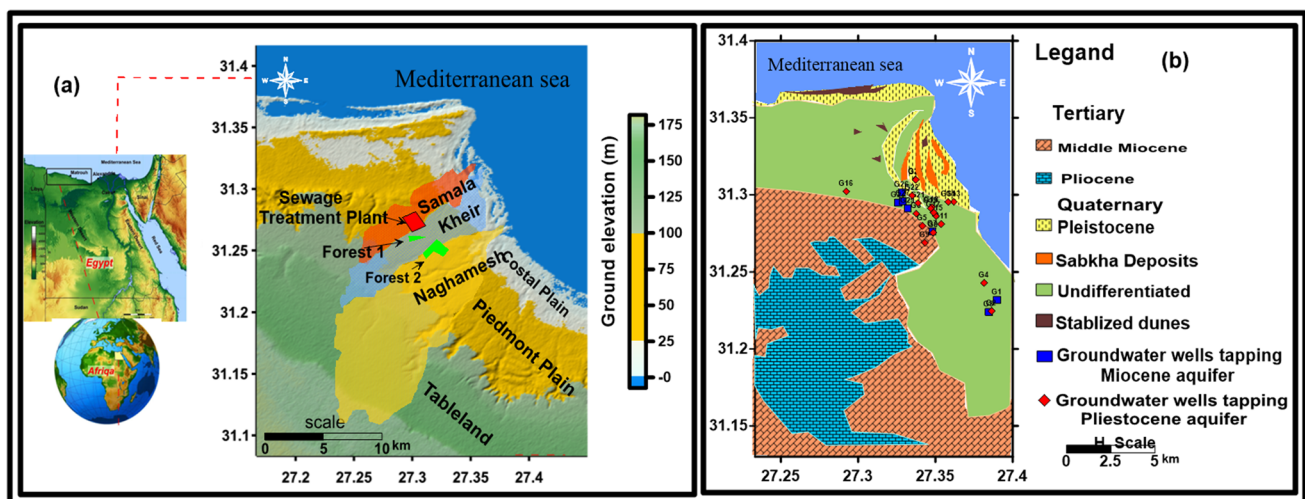


Fig. 1 a Location map of the study area. b Geological map of the study area with water point of groundwater samples

treatment plant provides 9 million m³/year of water to irrigate 4 km² of tree plantations. Groundwater interaction with polluted surface water can potentially put groundwater sources at risk. Different geochemical processes may affect ground water quality, including natural and anthropogenic activity. The study area is considered as a part of the south Mediterranean region where it is characterised by a moderate climate. The typical monthly maximum air temperature is 29.6 °C in August and 8.9 °C in January, with an average annual air temperature of 19.4 °C. The month of July has the highest relative humidity (73%) and the month of March has the lowest (63%) (Barseem et al. 2013). The evaporation rate records its maximum peaks in summer time (June–August). Wind speed ranges from 15.01 km/h in October to 22.04 km/h in January, resulting in 2420 mm of pitch evaporation per year (Masoud 2000). Rainfall starts from October to March, while the summer season is almost dry. The average annual rainfall varies from 64 to 412 mm (CLAC 2015), with an average annual cumulative precipitation of 155 mm. Many authors have researched the geomorphology, hydrology and geology of the coastal area of the northwest Mediterranean (Raslan 1995; Masoud 2000; Barseem 2006; Mohamed et al. 2011).

Geomorphologically, the northwestern Mediterranean coast is distinguished into three geomorphological units. These units were classified into the coastal plain, Piedmont plain and structural plateau (tableland) (Raslan 1995) (Fig. 1a). The elevation is between sea level and approximately 100 m in coastal and Piedmont plains. There were coastal dunes, ribs and sand dunes in the coastal plain. At the foot of the structural plateau, the Piedmont plain is growing. It has thick fine deposits of calcareous grounds derived from the alluvial deposits of various wadis. The main catchment region of the drainage line is the structural plateau (tableland). The construction of the plateau ranges from 100 to 175 m from the south to the north side of the Piedmont.

The geology of the study area has a considerable impact on the occurrence and quality of groundwater. The research region is covered with Tertiary and Quaternary sediments. The former includes sediments from the Middle Miocene (Marmarica Formation) to Pliocene. The Middle Miocene layers are made mainly of fossiliferous chalky and dolomitic limestone with marl and clay intercalations (El Shazly 1964; Yousif et al. 2014). In the studied area, Pliocene sediments have a limited distribution (El Shazly 1964; Hammad 1966). The Quaternary sediments contain Pleistocene and Holocene deposits. Pleistocene deposits are made up of oolitic limestone, which is composed of oolitic grains coupled with quartz sands and shell pieces bonded together by fine calcium carbonate. A variety of unconsolidated deposits, such as alluvial, aeolian and sabkha deposits, make up the Holocene deposits. Alluvial deposits are made up of muddy sands, silt and clay, and are rich in carbonate grains, rock pieces and

gravel. Quartz sands make to the carbonaceous composition of coastal dunes (Fig. 1b). Based on Hammad 1966, 1972, the Marmarica fractured limestone comprises carbonate minerals, including dolomite and calcite with minor clay and silicate minerals. The Quaternary oolitic limestone of marine origin has been formed along with the transgression and regression of shoreline of the Mediterranean (Zeuner 1959; Butzer 1959; El Shazly 1964; Hammad 1966).

Hydrogeological, Pleistocene and Middle Miocene aquifers are the major productive aquifers in the study area (Raslan 1995). The aquifer Pleistocene is composed of oolitic calcareous sand with shale interbeds. The groundwater of the oolitic aquifer occurs in a porous media under unconfined condition. The main recharge for the aquifer from the local annual rainfall and runoff water that comes from the upstream tableland plateau located in the southern side (Eissaa et al. 2018). The groundwater of the Middle Miocene is (Marmarica limestone) intercalated with alternate clay beds and groundwater occurs in fractured media where recharge rainwater percolates through joints and fissures (Mustafa et al. 2016). Hydrogeological cross-sections A–A' reveal that groundwater level in the Pleistocene aquifer flows from the upstream at southern side towards the Mediterranean at the northern downstream side. The locations of the two hydrogeological cross-sections in the study area help clarify local and regional landforms. The X–X' cross-section illustrates the various stages of the tableland and the scarp with its foot slope. Terraces were reported in the A–A' cross-section, which depicts a valley running through the tableland (Fig. 2) (Yousif et al. 2014). These aquifers are recharged by direct rainfall infiltrations and/or surface discharge (Sewidan 1978; NARSS. 2005). In the Pleistocene aquifer, the total depth of the wells ranges between 8 and 25 m, the depth to water ranges between 2 and 10 m, and TDS concentrations range between 8590 and 19,410 mg/l. On the other hand, in the Miocene aquifer, the total depth of the wells ranges between 23 and 42 m, the depth to water varies between 12 and 35 m, and TDS concentrations range between 4290 and 7920 mg/l (Table 3).

Materials and methods

Fieldwork began in June 2019 with an inventory survey of 31 existing water samples. These water samples were collected in 250-ml pre-washed polyethylene bottles with deionised water. The samples were kept at 4 °C in the laboratory to prevent microbial changes in water chemistry. The samples were geo-referenced using GPS (Trimble, Juno S-3 model). These samples are represented by 6 surface water samples and 25 groundwater samples (Fig. 3a). Samples were analysed at the hydrogeochemistry department of Desert Research Center (DRC) according to the methods adopted by the United States Geological

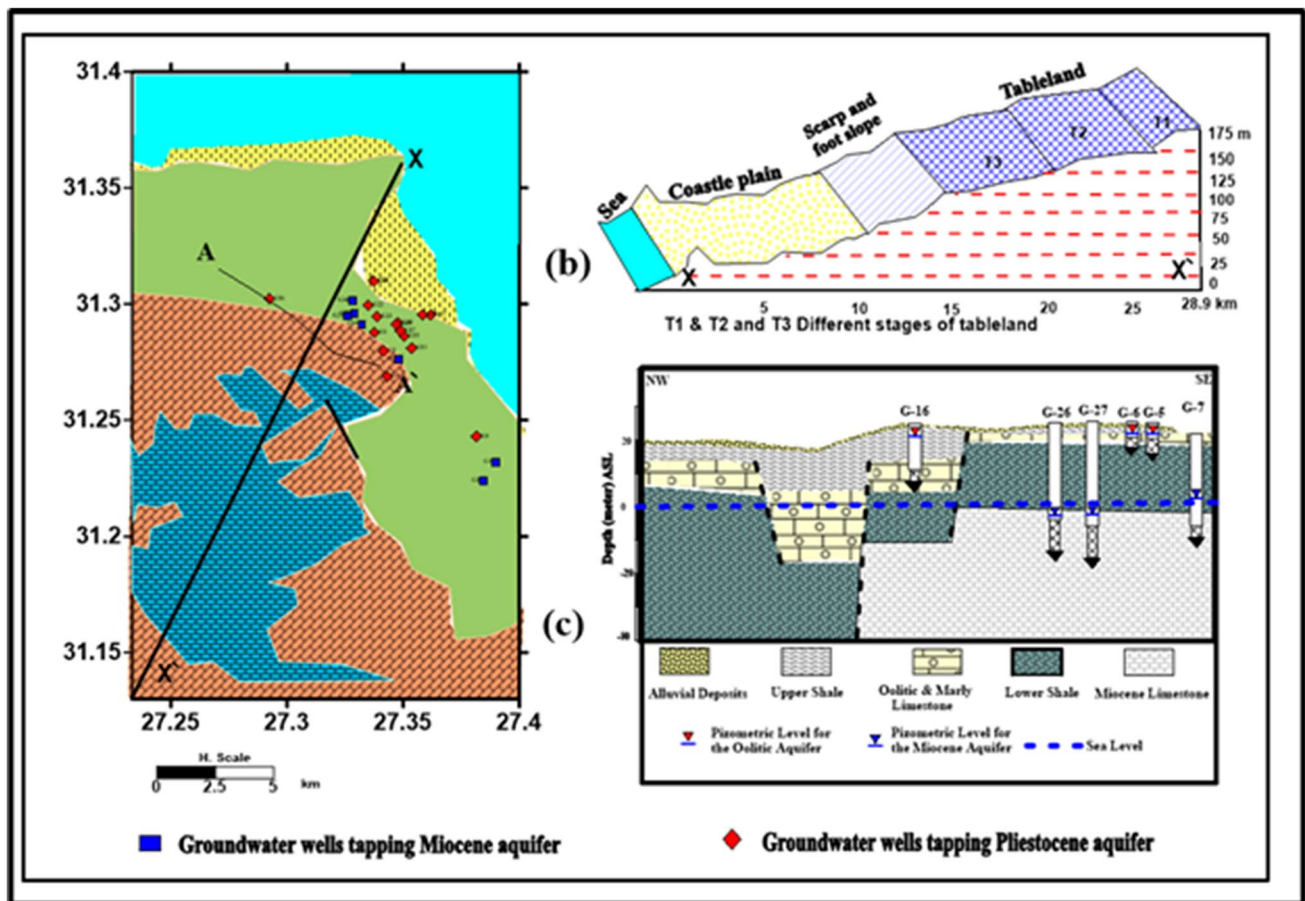


Fig. 2 Hydrogeological cross-section of the study area clarifies local and regional landforms with the locations of the two cross sections. **b** X–X' cross-section shows the different stages of tableland and the

scarp with its footslope. **c** A–A' Hydrogeological cross-section showing the piezometric level in the oolitic and Miocene fractured aquifer in the study area (modified after Al-Sayed et al. 2016)

Survey (Rainwater and Thatcher 1960; Fishman and Friedman 1989) and American Society for Testing and Materials (ASTM 2002). Sodium (Na^+) and potassium (K^+) were determined by flame photometer. Calcium (Ca^{2+}) and magnesium (Mg^{2+}) were determined by titration against (Na_2EDTA) by complexometric method. Carbonate (CO_3^{2-}) and bicarbonate (HCO_3^-) were determined by titration against sulphuric acid using the neutralisation method. Chloride (Cl^-) was determined volumetrically by titration against silver nitrate. Sulphate (SO_4^{2-}) was determined by the turbidity method using a double beam spectrophotometer. Trace element contents (Al^{3+} , Cd^{2+} , Cr^{3+} , Cu^+ , Fe^{2+} , Mo^{2+} , Mn^{2+} , Ni^{2+} , Pb^{2+} , V^{5+} and Zn^{2+}) of the water samples were determined using inductively coupled argon plasma (ICP). The obtained chemical data are expressed in milligrams per litre (mg/l) (Tables 1, 2, 3, and 4). Some parameters including the depth to water, total well depth, pH, temperature, EC, CO_3^{2-} , HCO_3^- , TOC, COD and NO_3^- were determined in situ using pH, EC meter, 3510 Jenway—UK, for CO_3^{2-} , HCO_3^- titrimetrically against sulphuric acid by neutralisation and measure of TOC, COD

and NO_3^- by using compact photometer PF-12Plus (Macherey–Nagel GmbH & Co. KG, filter photometer). Each sample was run twice and standards were checked for each sample in order to ensure analytical quality control.

The error % = $[\sum \text{Cations} - \sum \text{Anions}] / [\sum \text{Cations} + \sum \text{Anions}]$ was less than 5%.

Multivariate statistical analysis

All mathematical and statistical calculations were implemented using SPSS version 16.0 software to carry out the statistical analysis of the data; the data sets were log-transformed to accommodate a wide range of parameters (Matiatos et al. 2014).

Cluster analysis

The objective of cluster analysis is to group several objects to such an extent that they are more similar to one another in the same group (called a cluster) (Otto et al. 1998).

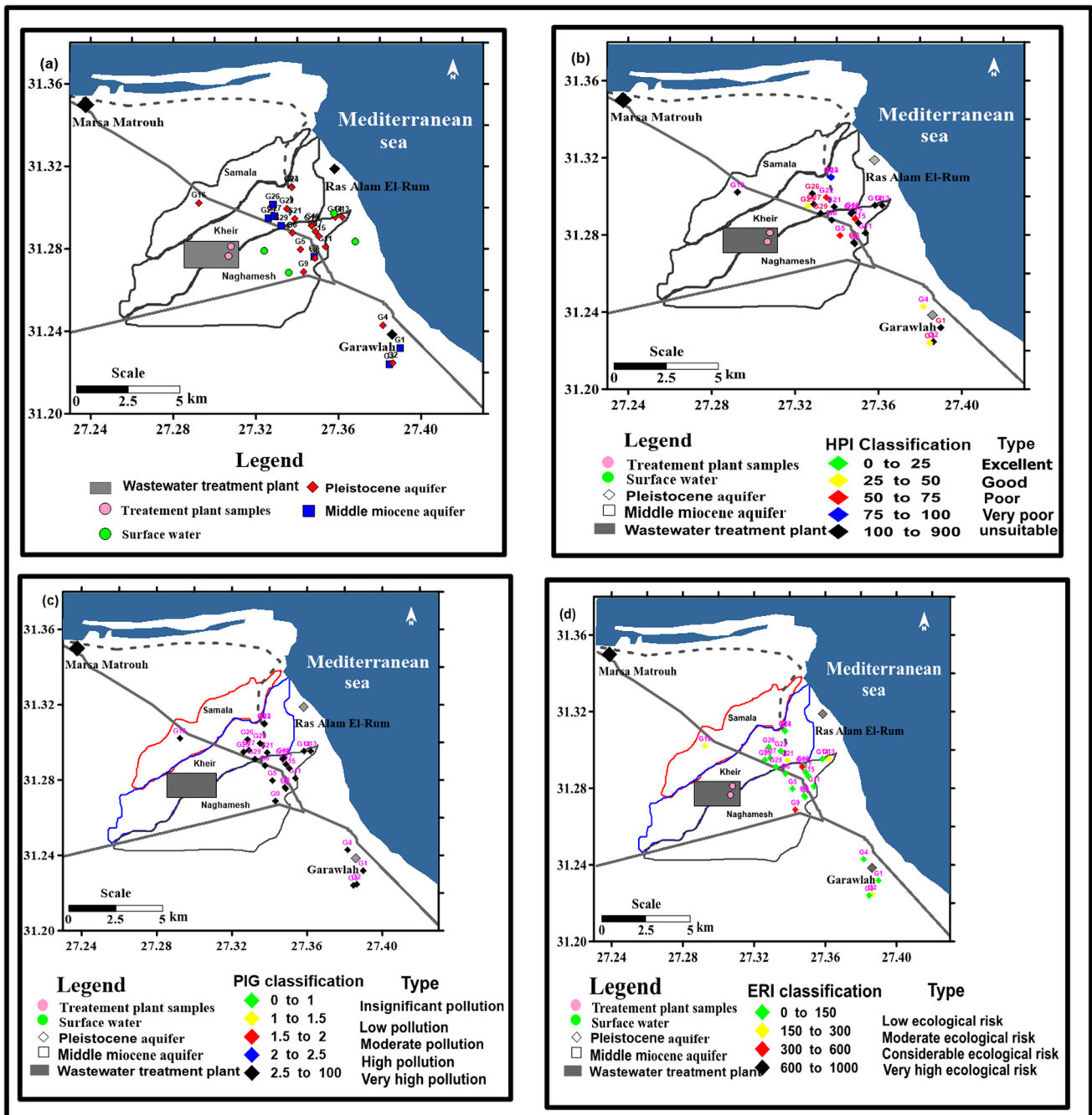


Fig. 3 a Map of sampling points of the area under investigation. b Heavy metal pollution index classification map of groundwater samples in the area under investigation. c Pollution index classification

map for the groundwater samples in the study area. d Classification map of ecological risk index of the studied groundwater in Pleistocene and Miocene aquifer

Principal component analysis/factor analysis

Factor analysis (FA) is a way used to analyse variability between observable and correlated variables as a result of a potentially lower range of variables termed factors (Shrestha and Kazama 2007). The correlations between the physico-chemical characteristics and the sample

locations were investigated using principal component analysis (PCA). According to Bartlett’s and KMO’s tests, the statistical significance of PCA was determined. For optimum variable participation, the varimax rotation technique was also used (Matiatos et al. 2014). The principal components (PCs) connected the parameters and sample locations in terms of factor loadings and factor scores.

Table 1 Unit weightage (W_i) and standard permissible value (S_i) in mg/l according to Egypt Guidelines according to the Minister of Health decree number 108 for 1995 and 458 for 2007

Item	Egyptian 2007	W_i Egy
Al ³⁺	0.1	0.01
Cd ²⁺	0.003	0.60
Cr ³⁺	0.05	0.04
Cu ⁺	2	0.0009
Fe ²⁺	0.3	0.01
Mo ²⁺	0.07	0.03
Mn ²⁺	0.4	0.00
Ni ²⁺	0.02	0.09
Pb ²⁺	0.01	0.18
V ⁵⁺	0.05	0.04
Zn ²⁺	3	0.0006

If an eigenvalue is less than 1, it is kept in the model (Kaiser 1974).

Pollution indices

Heavy metal pollution index

Heavy metal pollution index (HPI) is a comprehensive tool used for overall water quality determination, according to calculated weights of each metal; HPI was calculated according to Horton (1965) and Mohan et al. (1996). HPI is classified into five classes as follows: excellent, extended from 0 to 25; good, ranged from 26 to 50; poor, ranged from 51 to

Table 2 Assigned weight (w_i) and relative weight (W_i) of water quality parameters according to WHO (2017)

Parameter	Relative weight (Rw)	Weight parameter (Wp)	WHO (2017) Standard limits
pH	3	0.0577	7
Na ⁺	4	0.0769	200
K ⁺	1	0.0192	12
Ca ²⁺	2	0.0385	75
Mg ²⁺	2	0.0385	50
Cl ⁻	4	0.0769	250
HCO ₃ ⁻	3	0.0577	250
SO ₄ ²⁻	5	0.0962	250
NO ₃ ⁻	5	0.0962	50
Fe ²⁺	4	0.0769	0.3
Zn ²⁺	4	0.0769	3
Ni ²⁺	5	0.0962	0.02
Cr ³⁺	5	0.0962	0.05
Pb ²⁺	5	0.0962	0.01
Cd ²⁺	3	0.093	0.003
Cu ⁺	2	0.062	0.05
Mn ²⁺	3	0.093	0.05

75; very poor, ranged from 76 to 100; unsuitable, more than 100. It was calculated according to the following equation:

$$\text{HPI} = (\sum W_i \times Q_i) / \sum W_i \quad (i = n) \quad (1)$$

W_i is the unit weightage of the heavy metal i (Table 1), n is the number of heavy metals and Q_i is the sub-index of the heavy metal.

$$W_i = k/S_i \quad (2)$$

Here, k is the proportionality constant; S_i is the standard permissible limit of the heavy metal.

$$k = 1 / \sum S_i \quad (3)$$

S_1, S_2, S_3 and S_i represent standards for different heavy metals in the groundwater samples (Table 1).

$$Q_i = 100 \times (V_i/S_i) \quad (4)$$

V_i is the monitored value of the i parameter (mg/l).

Nitrate pollution index

Nitrate sources in the groundwater are classified to point sources such as irrigation of land by sewage effluents and nonpoint sources such as densely populated sanitation and intense farming practices (McLay et al. 2001). The nitrate pollution index (NPI) for the water samples was determined by Obeidat et al. (2012). The water quality according to NPI values was classified into five types: clean (unpolluted) ($\text{NPI} < 0$); light pollution ($0 < \text{NPI} < 1$); moderate pollution ($1 < \text{NPI} < 2$); significant pollution ($2 < \text{NPI} < 3$); very significant pollution ($\text{NPI} > 3$). The NPI for the water samples was determined by using the following relation:

$$\text{NPI} = (C_s - \text{HAV}) / \text{HAV}$$

where C_s is the analytical concentration of nitrate, and HAV is the threshold value of anthropogenic source (human affected value) taken as 50 mg/l.

Pollution index of groundwater

Drinking water quality can be assessed with the use of pollution index of groundwater (PIG) (Rao 2012), and were utilised successfully in several locations to monitor and evaluate variations in drinking water quality (Rao et al. 2018; Rao and Chaudhary 2019). In the current study, the PIG values for each water sample were calculated using the standard limit of the World Health Organization (WHO 2017) prescribed for safe drinking water (Table 2). All the observed chemical variables in each sample of groundwater are determined in the PIG values. Thus, the effects of

Table 3 Physiochemical parameters for groundwater and surface water samples

No	TD	DW	pH	TDS	TH	Na ⁺	K ⁺	SO ₄ ²⁻	Cl ⁻	NO ₃ ⁻	PO ₄ ³⁻	BOD	COD	TOC
Pleistocene aquifer (mg/l)														
G2	24	10	7.2	6438	1499	1750	55	1405	2622	3.7	Nil	20	14	101
G4	20	4	7.2	8710	2743	1900	57	2650	3085	5.9	Nil	2.5	50	218
G5	18	5	7.6	6365	1307	1900	100	800	3085	2.8	Nil	7.5	57	336
G6	12	7	8	5041	1218	1450	52	650	2417	2.5	3.06	27.5	21	67
G8	22	5	7.9	7338	1374	2300	71	480	3959	6.6	Nil	Nil	57	17
G9	8	10	7.9	5955	1250	1700	70	1500	2211	1	5.02	7.5	57	50
G11	25	9	7.2	7627	1464	2350	54	900	3754	8.7	Nil	15	57	Nil
G13	9	2	7.5	8285	1672	2550	80	727	4319	8.1	Nil	Nil	43	168
G14	20	2	7.7	8276	1298	2650	100	824	4216	4.4	2.8	2.5	28	34
G15	23	4	7.4	9007	1835	2600	66	730	4936	4.2	Nil	10	85	50
G16	24	6	8.1	6163	953	2000	55	473	3239	1	Nil	2.5	43	Nil
G17	17	7	7.3	5747	1337	1650	55	344	3188	12.2	9.8	Nil	36	118
G18	15	5	7.7	9458	2360	2500	70	1000	5039	3.2	8.9	10	78	Nil
G19	25	6	7.9	9489	1856	2750	100	850	5142	3.5	Nil	40	43	34
G21	12	5	7.3	7565	1711	2100	66	972	3805	1.5	8.08	2.5	71	269
G22	23	8	7.6	11,741	2359	3500	100	1212	6067	1	Nil	Nil	71	Nil
G23	10	8	7.3	10,489	2548	2700	76	2150	4628	1.4	12.3	15	71	Nil
G24	14	4	7.3	9420	2907	2150	65	1950	4216	1.6	Nil	37.5	57	84
Miocene aquifer (mg/l)														
G1	25	12	7.1	3483	1439	580	50	1340	951	9.2	Nil	22.5	14.2	50
G3	37	30	7.4	3863	817	1160	45	460	1851	2.4	Nil	35	14.2	168
G7	23	15	7.6	2360	805	600	32	140	1260	1.0	Nil	Nil	35.6	50
G25	26	14	7.5	4263	844	1300	41	459	2057	2.7	11.7	25	85.44	1092
G26	39	30	7.2	2635	1026	580	36	159	1363	7.1	Nil	25	14.2	34
G27	42	35	7.3	4742	984	1380	42	726	2160	2.8	Nil	35	42.72	86
G29	28	17	7.4	4398	1094	1160	55	470	2262	3.8	4.31	10	42.72	34
Surface water (mg/l)														
S10	-	-	8.3	2455	450	740	28	400	1054	3.2	1.1	438	21	52
S12	-	-	7.1	36,758	3828	12,000	200	4144	19,025	1.0	23.7	100	712	202
S20	-	-	8.2	41,958	3911	13,400	600	6000	20,567	1.0	1.7	125	285	386
S28	-	-	7.7	10,397	1219	3550	100	904	5142	1.0	9.9	138	85	103
Treatment plant (before)	-	-	7.1	9608	803	3300	150	529	5142	13.2	12.9	238	57	240
Treatment plant (after)	-	-	7.5	4510	1325	1220	65	420	2160	3.1	23.5	288	50	51
Permissible limit WHO (2017)	-	-	6.5–8.5	1000	200	200	-	500	250	50	0.1	-	-	-

pH is in numerical value, EC is in µS/cm; all others are in mg/l

chemical pollution on the aquifer system are distinct. PIG calculation involves four steps which are determined according to Rao (2012):

$$W_p = R_w / \sum R_w \tag{5}$$

$$S_c = \frac{C}{D_s} \tag{6}$$

$$O_w = w_p \times S_c \tag{7}$$

$$PIG = \sum O_w \tag{8}$$

Ecological risk index

In consideration of the pollution and toxic response factor, the potential ecological index (ERI) for the heavy metals analysed has been quantitatively assessed. In the present study, the ERI for each groundwater sample was calculated using Eq. 9 and Eq. 10:

Table 4 Heavy metal analysis for groundwater and surface water samples, all concentrations (mg/l)

No	Al ³⁺	Cd ²⁺	Cr ³⁺	Cu ⁺	Fe ²⁺	Mo ²⁺	Mn ²⁺	Ni ²⁺	Pb ²⁺	V ⁵⁺	Zn ²⁺
Pleistocene aquifer (mg/l)											
G2	2.105	0.0191	<0.01	2.526	<0.02	<0.001	0.1363	<0.002	0.0482	0.0335	<0.0006
G4	0.0991	<0.0006	<0.01	0.0590	<0.02	<0.001	0.0045	<0.002	<0.008	<0.01	<0.0006
G5	0.0862	<0.0006	<0.01	0.0761	<0.02	0.0537	0.0064	0.0397	0.0153	<0.01	<0.0006
G6	0.2037	<0.0006	<0.01	0.6749	<0.02	<0.001	0.0146	<0.002	0.1579	<0.01	<0.0006
G8	0.1481	<0.0006	<0.01	0.3304	<0.02	0.0241	0.0081	<0.002	0.0858	0.0291	<0.0006
G9	0.2854	0.0204	<0.01	0.9583	<0.02	0.0296	0.0184	<0.002	0.3053	0.0290	<0.0006
G11	0.0324	0.0134	<0.01	0.0012	<0.02	0.1182	<0.002	<0.002	0.0168	<0.01	<0.0006
G13	0.3372	0.0119	<0.01	0.5047	<0.02	0.0583	0.0301	<0.002	0.0889	<0.01	<0.0006
G14	0.2011	0.0072	<0.01	0.5012	<0.02	0.0630	0.0184	<0.002	<0.008	<0.01	<0.0006
G15	0.0417	0.0083	<0.01	0.0265	<0.02	<0.001	0.0030	<0.002	<0.008	<0.01	<0.0006
G16	0.0653	0.0212	<0.01	0.0229	<0.02	0.0171	0.0036	0.0311	<0.008	<0.01	<0.0006
G17	0.4775	<0.0006	<0.01	1.254	<0.02	0.0140	0.0803	0.0269	<0.008	<0.01	<0.0006
G18	0.0033	<0.0006	<0.01	0.1263	<0.02	<0.004	0.0034	0.0109	0.0764	<0.01	<0.0006
G19	0.0707	0.0270	<0.01	0.0589	<0.02	0.0615	<0.002	<0.002	0.1642	0.0284	<0.0006
G21	0.1093	0.0171	0.0371	3.369	<0.02	<0.001	0.0240	<0.002	0.2034	<0.01	<0.0006
G22	1.752	<0.0006	0.0312	3.088	<0.02	<0.001	0.1416	0.0070	<0.008	0.0210	<0.0006
G23	0.0663	0.0009	0.0209	0.0251	<0.02	<0.001	0.0030	0.0580	0.0780	<0.01	<0.0006
G24	0.2026	<0.0006	0.0203	0.6892	<0.02	0.1486	0.0147	0.0109	0.0278	0.0753	<0.0006
Miocene aquifer (mg/l)											
G1	1.748	9.434	<0.01	0.0106	<0.02	<0.001	10.24	0.1328	<0.008	<0.01	0.2567
G3	1.643	1.112	<0.01	<0.006	<0.02	<0.001	11.30	<0.002	0.01	0.1097	0.0354
G7	0.9865	1.007	<0.01	<0.006	<0.02	0.0247	12.38	<0.002	0.0272	0.0591	0.0402
G25	2.126	0.0545	<0.01	<0.006	<0.02	<0.001	5.484	<0.002	0.01	<0.01	0.0113
G26	0.718	0.2161	<0.01	0.0131	<0.02	0.0172	7.924	0.0999	0.0999	0.0475	<0.006
G27	2.658	0.0695	0.01	0.01	<0.02	0.0335	10.41	0.1046	0.1046	<0.01	0.0097
G29	1.858	0.1247	<0.01	<0.006	<0.02	0.0154	10.24	0.1328	0.1171	<0.01	0.2567
Surface water (mg/l)											
S10	<0.01	1.5	<0.01	2.6	0.1290	0.0109	3.2	0.2018	1.2	<0.01	0.0080
S12	<0.01	1.78	0.0517	2.4	0.1924	0.0653	2.4	0.1156	1.03	0.0653	2.902
S20	<0.01	2.6	0.3403	2.3	0.1764	0.0521	1.5	<0.002	2.01	0.0521	0.4242
S28	<0.01	3.1	0.0527	2.5	0.2511	<0.001	1.6	<0.002	1.04	<0.01	0.0687
Treatment plant (before)	<0.01	3.4	0.1763	2.1	0.1094	0.0568	2.5	<0.002	1.11	0.0568	0.0786
Treatment plant (after)	<0.01	2.5	0.6108	1.3	0.1085	<0.001	1.9	<0.002	1.01	<0.01	0.0553
Permissible limit WHO (2017)	2.9	0.003	0.05	0.05	0.3	0.1	0.1	0.2	0.01	0.5	3

$$ERI = \sum RI = \sum TiXPi \quad (9)$$

$$PI = \frac{Cs}{Cb} \quad (10)$$

where RI is the potential ecological risk factor of each heavy metal, Ti is the toxic-response factor of heavy metal, PI is the pollution index, Cs is the concentration of heavy metals in the sample and Cb is the corresponding background values. The toxic-response factor of heavy metals is given as Cd = 30; Co, Cu, Ni and Pb = 5; Fe, Cr, Zn and Mn = 1

(Bhutiani et al. 2017; Adimalla and Wang 2018; Taiwo et al. 2019).

Hydrochemical facies evolution of groundwater

The evolution diagram for hydrochemical facies, proposed by Giménez-Forcada (2010), offers a convenient manner of recognising the status of aquifers in temporal intrusion/refreshing phases, which is identified through the distribution of anion and cation levels in the square diagram (Fig. 4a). Three heteropic facies are identified in this plot:

Na–Cl (sea water), Ca–HCO₃ (fresh water) and Ca–Cl (water salinized with direct bases exchange).

Water quality for irrigation purpose

Water quality assessment for irrigation is an essential technique for sustainable development as it gives essential information for water management. To classify the water into irrigation water categories, the first utilises sodium percentage (Na %), although it also uses sodium adsorption ratio (SAR) (Richards 1954; Wilcox 1955). Sodium percentage is

calculated by dividing the sum of Na⁺ and K⁺ concentrations by total cations (Eq. 11; Raghunath 1987). SAR is calculated as the ratio between Na⁺ and the square root of the average of Ca²⁺ and Mg²⁺ concentrations (Eq. 12; Richards 1954). For both calculations, the ion concentrations (mEq/l) are used.

$$Na\% = \frac{(Na + +K+)x100}{(Ca2 + +Mg2 + +Na + +K+)} \tag{11}$$

$$SAR = Na + +\sqrt{Ca2 + +Mg2 + /2} \tag{12}$$

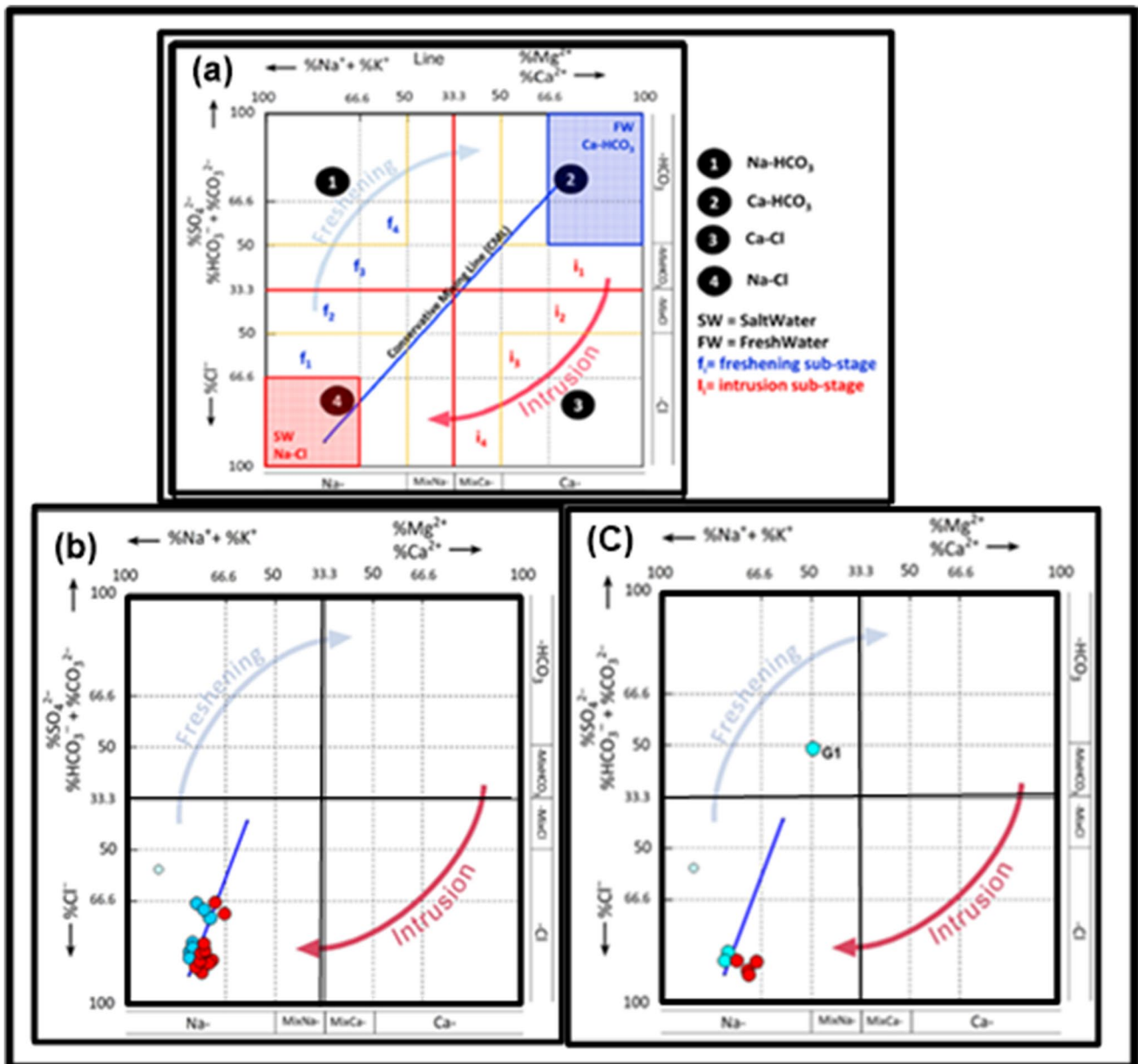


Fig. 4 a Hydrochemical facies evolution diagram (HFE-D) (Gimenez-Forcada 2010). b HFE diagram in groundwater of the Pleistocene aquifer and c HFE diagram in groundwater of Miocene aquifer

Results and discussion

Hydrogeochemistry

The hydrochemical data provides an overview of the physical–chemical parameters measured in the groundwater and surface water samples. Figure 5a, b shows the box plots of the water parameters, which indicate the fluctuations in the analysed parameter values. The pH values, ranged from 7.2 to 8.1 in the Pleistocene aquifer, from 7.1 to 7.6 in the Miocene aquifer and from 7.1 to 8.3 in surface water, reflected that the groundwater and surface water samples are somewhat neutral to slightly alkaline. The electric conductivity (EC) values represent water's dissolved salt content and higher values typically reflect higher concentrations of ions in the water (Prasanth et al. 2012). The EC values ranged from 8520 to 19,410 $\mu\text{S}/\text{cm}$ in the Pleistocene groundwater, from 4290 to 7920 $\mu\text{S}/\text{cm}$ in the Miocene groundwater and from 3970 to 64,410 $\mu\text{S}/\text{cm}$ in the surface water. The EC value differences are attributable to the composition of the aquifer rocks. The total dissolved solids (TDS) values ranged from 5041 to 11,741 mg/l in the Pleistocene aquifer, from 2360 to 4742 mg/l in the Miocene groundwater and from 2455 to 41,958 mg/l in the surface water. Major ions are observed in Na^+ and Cl^- correspondingly as prominent cation and anion species in both the groundwater and surface water sample concentrations. The concentration of Na^+ varies from 1450 to 3500 mg/l in the Pleistocene groundwater, from 580 to 1380 mg/l in the Miocene groundwater and from 740 to 13,400 mg/l in the surface water. The ionic concentration of Cl^- is highest among all the ions and the concentration of Cl^- in Pleistocene groundwater is

between 2211 and 6076 mg/l, in Miocene groundwater is between 951 to 2262 mg/l, and in surface water from 1054 to 20,567 mg/l. Both the surface water and the groundwater display significantly higher Na^+ and Cl^- concentrations, indicating that seawater most likely affects the water quality in the area under investigation and this indicates the mixing of groundwater with the matrix of marine aquifers. The concentration of K^+ shows the least variation with the range of 52 to 100 mg/l in the Pleistocene groundwater, from 32 to 55 mg/l in the Miocene groundwater and 28 to 600 mg/l in the surface water. In the Pleistocene groundwater, Ca^{2+} and Mg^{2+} concentrations range between 131–767 mg/l and 152–270 mg/l, respectively. Also, in the Miocene groundwater, Ca^{2+} and Mg^{2+} concentrations range between 129–306 mg/l and 113–164 mg/l. Similarly, the concentrations of SO_4^{2-} and alkalinity vary from 344 to 2650 mg/l and 50 to 205 mg/l in the Pleistocene groundwater, while in the Miocene groundwater they range from 140 to 1340 mg/l and 135 to 275 mg/l, in each case. The dissolving of marine sediments is the result of the high salinity of groundwater (Table 3). Also, to determine the hydrogeochemical characteristics of the research region, the analytical values were plotted on a Piper diagram (Piper 1944). The Piper trilinear diagram has two triangles, one for cations and the other for anions, as well as a diamond-shaped area for cations and anions together. Chemical analysis data (expressed in meq/l) of both major cations (Ca^{2+} , Mg^{2+} and $\text{Na}^+ + \text{K}^+$) and major anions (Cl^- , SO_4^{2-} and $\text{CO}_3^{2-} + \text{HCO}_3^-$) are plotted in the diamond shape. The plotting of different types of groundwater quality in different sub-areas of the diamond-shaped plot makes it easy to identify them. The data of the chemical analysis of groundwater are plotted on one diagram. Figure 6

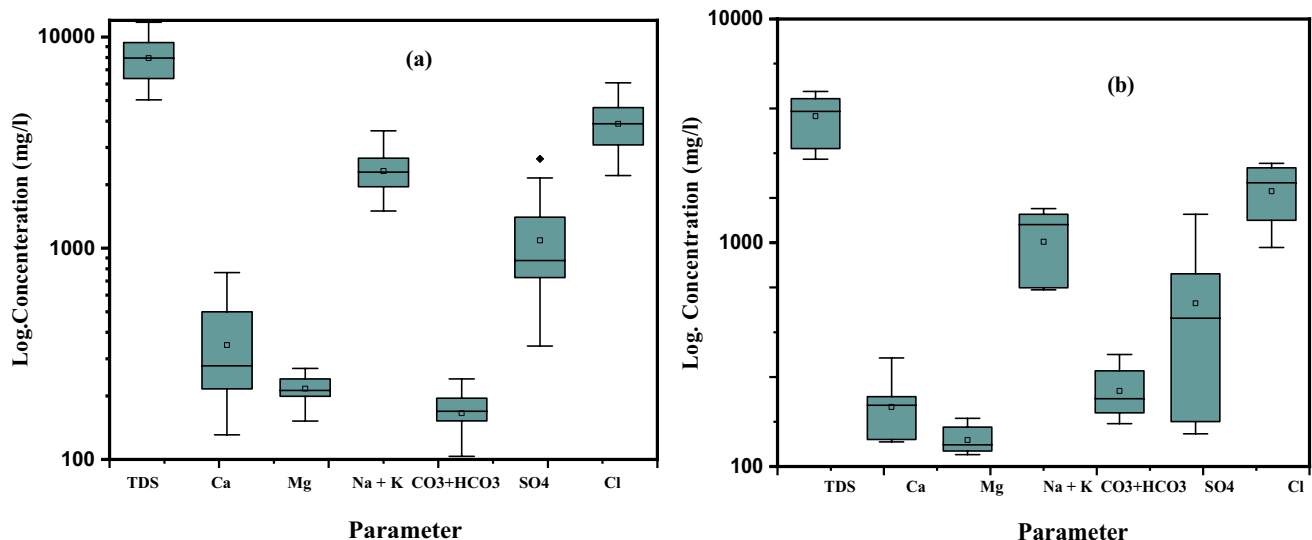
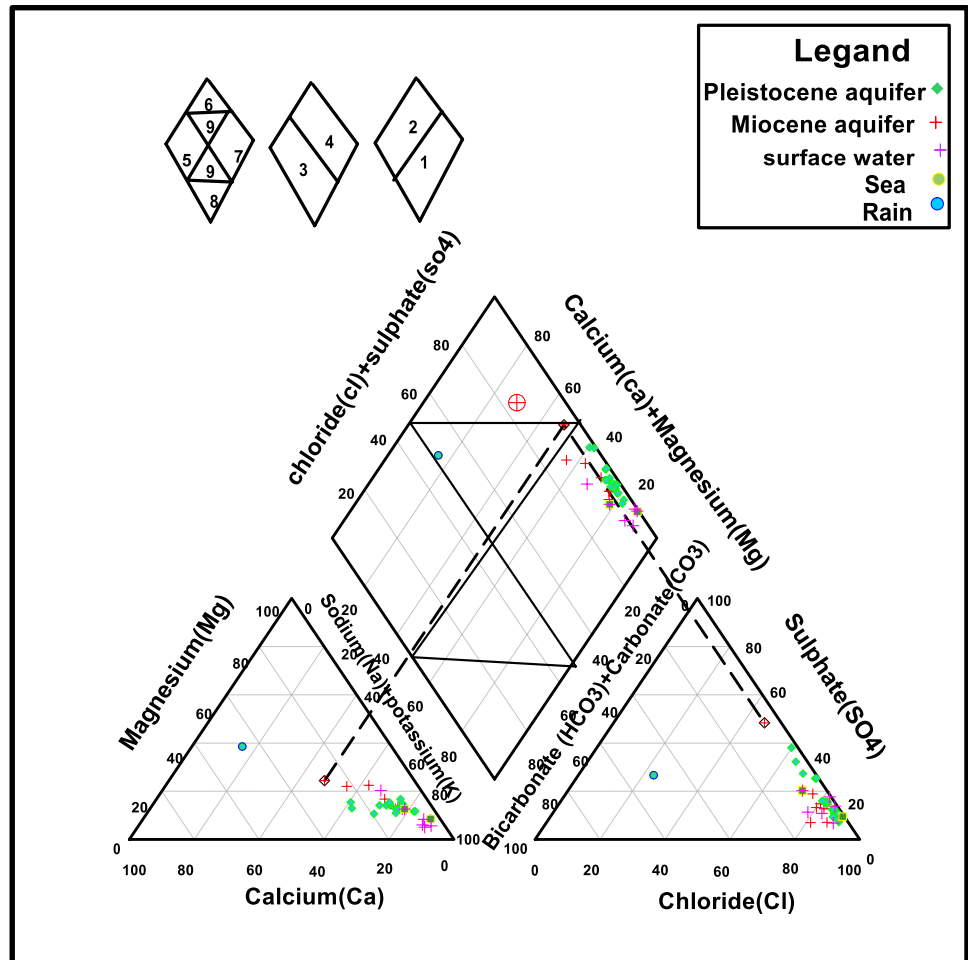


Fig. 5 Box plots of TDS, Ca, Mg, Na + K, CO₃+HCO₃, SO₄ and Cl in the Pleistocene aquifer (a) and the Miocene aquifer (b). All concentrations are given in milligrams per litre (mg/l)

Fig. 6 Piper diagram of the groundwater samples



shows that groundwater samples of Pleistocene and Miocene aquifers are located in sub-area 7, where the groundwater is dominated by noncarbonated alkali and strong acids (primary salinity) exceed 50%. This reflects that the main groundwater salinisation is mainly attributed to leaching and dissolution processes of aquifer matrix rich with minerals. The graphical method described by Stiff (1951) makes it possible to illustrate this evolution (Fig. 7). The use of a Stiff diagram allows the mapping of a polygon that assumes geometry based on hydrochemical element content and provides an estimate of the dominating species for each well. The three axes of the diagram are, from top to bottom, as follows: (1) $\text{Na}^+ - \text{K}^+ - \text{Cl}^-$; (2) $\text{Ca}^{2+} - \text{HCO}_3^- - \text{CO}_3^{2-}$; (3) $\text{Mg}^{2+} - \text{SO}_4^{2-}$. The use of Stiff diagrams allows for the chemical classification of waters determined by the presence of anion and cation facies. As shown in Fig. 8, higher Cl^- and Na^+ contents were measured in groundwater from G4 to G16 wells in Pleistocene aquifer and from G1 to G26 in Miocene aquifer. It may be determined that there is a lot of mixing of different water types in the study region, which is caused by marine intrusion that comes through groundwater resources and the mixing of groundwater with

the matrix of marine aquifers (Guesdon et al. 2016). The dominant water types that correspond to the groundwater sampled in wells were $\text{Na}^+ - \text{K}^+ - \text{Mg}^{2+} - \text{Cl}^-$. Except well no. G1, the water type is $\text{Na}^+ - \text{K}^+ - \text{Ca}^{2+} - \text{SO}_4^{2-}$. It can also be determined that the mixing of diverse water types in the research area is severe, caused by saltwater due to excessive groundwater abstraction (Sherif et al. 2006). A multi-rectangular hydrochemical facies evolution diagram (HFE) can be employed to determine the dynamics of marine intrusion, considering the percentages of major ions, showing the intruding and freshening phases. Figure 5b and c shows that the majority of samples are appropriate for a phase of marine intrusion. The Na–Cl facies signifies that the state of aquifer is probably controlled by water–rock interaction. The samples shown in HFE-D confirm the hypotheses regarding salinisation with the exception of one sample (G1), which is scattered in the field of freshening. The methodology of classification proposed in the present study takes into account that of Giménez-Forcada (2010).

For proper management of an aquatic environment, a water quality guideline must be defined. When settling on a water quality goal, the proposed use of water is taken into

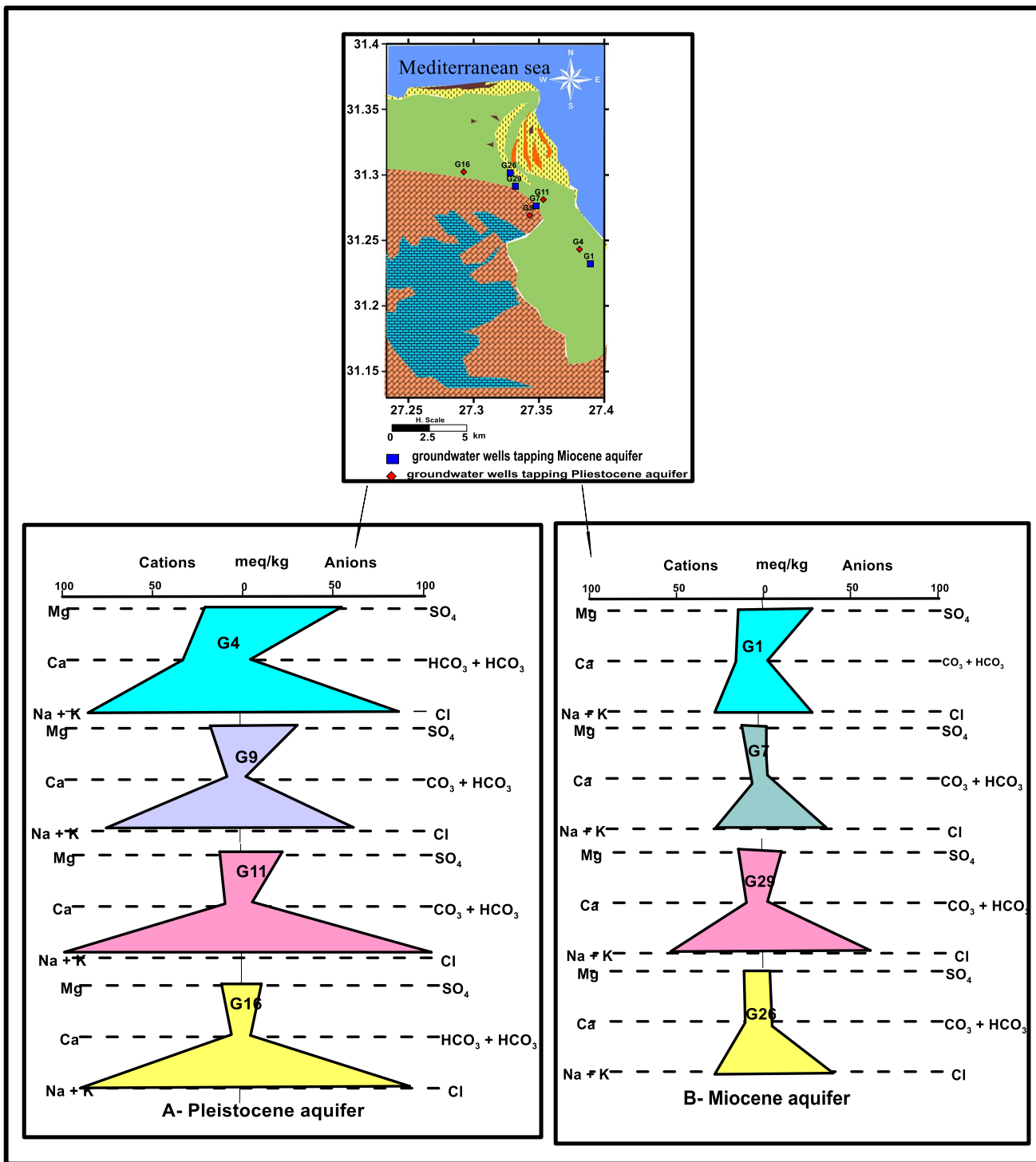


Fig. 7 Stiff diagram for the groundwater types

account. Table 3 lists the main physiochemical parameters measured, together with their WHO (2017) permissible limits for drinking purposes. The values of TDS, Cl⁻, SO₄²⁻, TH, TOC, PO₄³⁻, BOD, COD, and Na⁺ were found to be above permissible limits in the groundwater and surface

water according to WHO (2017). The high levels of contamination shown by the physiochemical parameters point is due to the mixing of groundwater with the matrix of marine aquifers, municipal sewage discharge from waste treatment plant in the study area, and land runoff. According to the

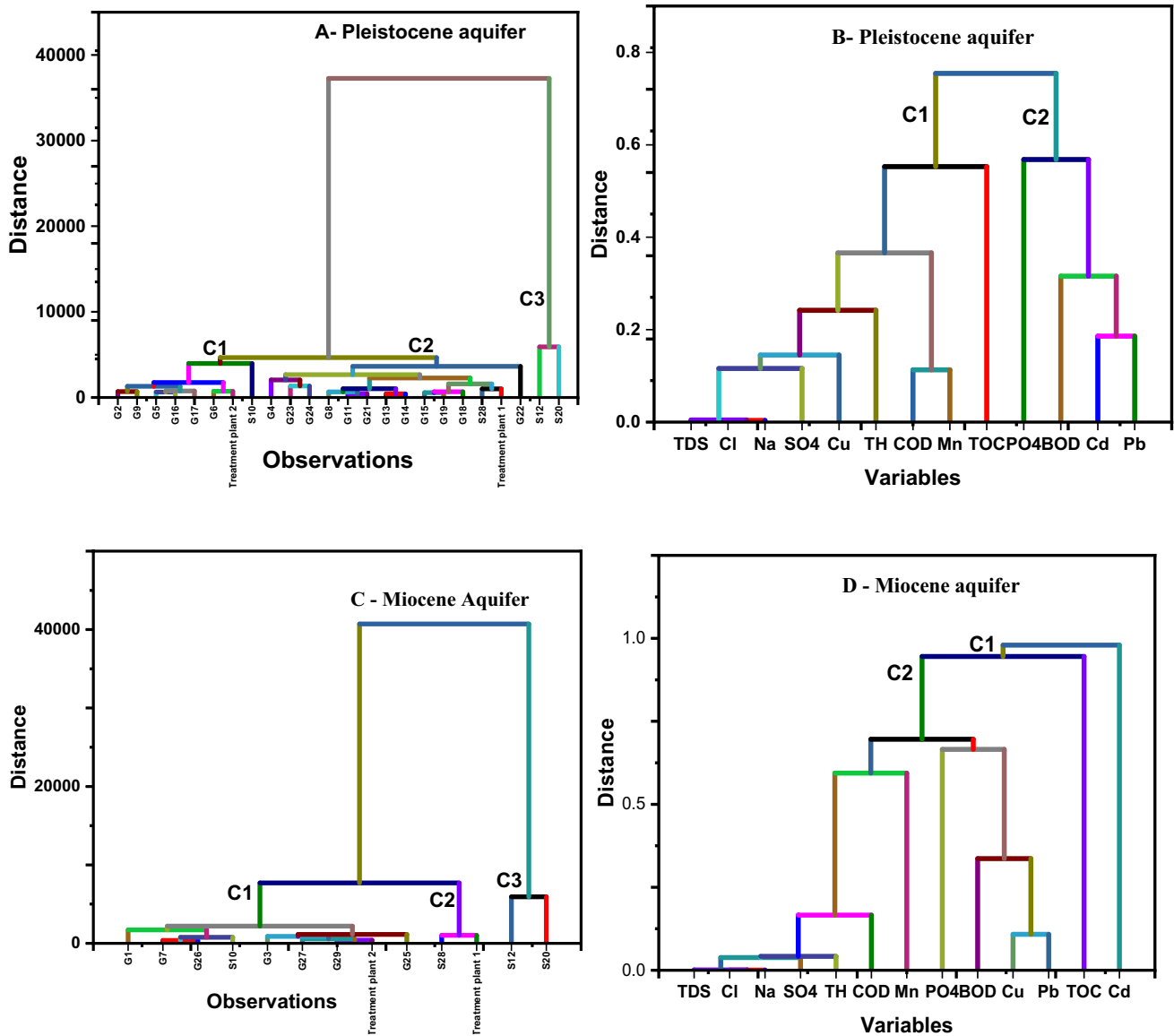


Fig. 8 Dendrogram based on agglomerative hierarchical clustering for Pleistocene aquifer and Miocene aquifer

World Health Organization (WHO 2017), high levels of PO_4^{3-} are responsible for nutrient enrichment of water bodies, and are contributed by detergent-containing residential wastewater and fertiliser land runoff. The COD and TOC values indicate that both oxidisable organic and inorganic pollutants have contaminated the water body (Mohamed et al. 2015). BOD values indicate poor water quality, which can be linked to waste discharges containing high levels of organic and nutrient content, as well as increased microbial activity owing to organic matter breakdown. The concentrations of several heavy metals that were analysed, as well as the permitted limits established by WHO (2017), are given in Table 4. The cadmium (Cd^{2+}) contents were found to be above the WHO’s permissible limit in eight Pleistocene

sites, four Miocene sites and four surface water sites. It ranges from ND to 9.434 mg/l, which could be attributed to wastewaters from the treatment plant. Chromium (Cr^{3+}), aluminium (Al^{3+}), molybdenum (Mo^{2+}), vanadium (V^{5+}), iron (Fe^{2+}) and zinc (Zn^{2+}) contents in all groundwater samples were within permissible limits. Copper (Cu^+) and lead (Pb^{2+}) concentrations, on the other hand, were both over permitted levels in some sample locations. The copper (Cu^+) contents range from ND to 3.369 mg/l in groundwater. The lead (Pb^{2+}) contents range from ND to 0.3053 mg/l in groundwater. Manganese (Mn^{2+}) is a secondary water pollutant, and the concentration of Mn^{2+} in groundwater samples was found to be over the permissible limit. It ranges from ND to 12.38 mg/l. High amounts of Mn^{2+} can cause

water to become black or brown and have a bitter metallic taste (Dutta et al. 2018). Heavy metal concentrations seen in the research region could be due to municipal sewage water and wastewater from a waste treatment plant.

Statistical analysis

Correlation of water parameters

In accordance with the database of 13 different variables, which includes TDS, TH, Cl^- , SO_4^{2-} , Na^+ , PO_4^{3-} , BOD, TOC, COD, Cd^{2+} , Cu^+ , Pb^{2+} and Mn^{2+} , we tried to figure out how sewage treatment plants affect groundwater. Table 5A shows the Pearson correlation matrix for the

Pleistocene aquifer. Total dissolved solids have a strong positive correlation with Cl^- , Na^+ , TOC, COD, Cu^+ , Pb^{2+} and Mn^{2+} . Total hardness showed strong and positive correlation with SO_4^{2-} , PO_4^{3-} and BOD. Chloride showed positive correlation with Na^+ , TOC, COD, Cd^{2+} , Cu^+ and Mn^{2+} . Sulphate showed positive correlation with PO_4^{3-} . Sodium showed positive correlation with TOC, COD, Cd^{2+} , Cu^+ , Pb^{2+} and Mn^{2+} . Pearson's correlation matrix is presented in Table 5B for the Miocene aquifer. A strong positive correlation was found between total dissolved solids with TH, Cl^- , SO_4^{2-} , Na^+ , Cu^+ , Pb^{2+} and COD. Total hardness showed a strong and positive correlation with Cl^- , SO_4^{2-} , Na^+ , COD, Cu^+ and Pb^{2+} . Chloride showed a positive correlation with SO_4^{2-} , Na^+ , COD, Cu^+ and Pb^{2+} . Sulphate showed a positive

Table 5 (A,B)Correlation matrix, Kaiser–Meyer–Olkin (KMO) and Bartlett's test results for 13 physico-chemical variables shortlisted for multivariate statistical analysis

A. Correlation matrix ^a in the Pleistocene aquifer													
	TDS	TH	Cl^-	SO_4^{2-}	Na^+	PO_4^{3-}	BOD	TOC	COD	Cd^{2+}	Cu^+	Pb^{2+}	Mn^{2+}
TDS	1.000												
TH	-0.116	1.000											
Cl^-	0.979	-0.303	1.000										
SO_4^{2-}	0.437	0.797	0.250	1.000									
Na^+	0.969	-0.310	0.994	0.215	1.000								
PO_4^{3-}	-0.365	0.945	-0.543	0.653	-0.558	1.000							
BOD	0.034	-0.789	0.188	-0.649	0.191	-0.766	1.000						
TOC	0.510	-0.300	0.554	-0.007	0.568	-0.428	0.081	1.000					
COD	0.842	-0.190	0.859	0.236	0.840	-0.401	0.078	0.349	1.000				
Cd^{2+}	0.411	-0.817	0.554	-0.502	0.557	-0.874	0.738	0.368	0.343	1.000			
Cu^+	0.874	-0.385	0.899	0.166	0.900	-0.576	0.240	0.568	0.631	0.615	1.000		
Pb^{2+}	0.607	-0.763	0.723	-0.310	0.728	-0.870	0.742	0.457	0.458	0.895	0.795	1.000	
Mn^{2+}	0.636	-0.434	0.711	-0.083	0.695	-0.577	0.430	0.241	0.892	0.442	0.490	0.551	1.000
Kaiser–Meyer–Olkin (KMO) measure of sampling adequacy 0.557													
Bartlett's test of sphericity significance 0.000													
B. Correlation matrix ^a in the Miocene aquifer													
	TDS	TH	Cl^-	SO_4^{2-}	Na^+	PO_4^{3-}	BOD	TOC	COD	Cd^{2+}	Cu^+	Pb^{2+}	Mn^{2+}
TDS	1.000												
TH	0.963	1.000											
Cl^-	0.999	0.957	1.000										
SO_4^{2-}	0.969	0.962	0.957	1.000									
Na^+	0.999	0.952	0.999	0.959	1.000								
PO_4^{3-}	0.319	0.333	0.343	0.167	0.335	1.000							
BOD	0.028	-0.087	0.031	-0.016	0.044	0.314	1.000						
TOC	0.171	0.100	0.170	0.161	0.178	0.207	-0.165	1.000					
COD	0.845	0.857	0.861	0.755	0.850	0.554	-0.018	0.145	1.000				
Cd^{2+}	0.059	0.146	0.032	0.174	0.043	-0.004	0.077	-0.206	-0.033	1.000			
Cu^+	0.927	0.871	0.916	0.922	0.926	0.227	0.144	0.128	0.639	0.105	1.000		
Pb^{2+}	0.699	0.575	0.695	0.656	0.710	0.366	0.669	0.010	0.440	0.149	0.817	1.000	
Mn^{2+}	0.338	0.422	0.355	0.306	0.333	0.115	-0.240	-0.159	0.683	-0.099	0.035	-0.169	1.000
Kaiser–Meyer–Olkin (KMO) measure of sampling adequacy 0.444													
Bartlett's test of sphericity significance 0.000													

correlation with Na^+ , COD, Cu^+ and Pb^{2+} . Sodium showed a positive correlation with COD, Cu^+ and Pb^{2+} . Total hardness showed a strong positive correlation with Cl^- , SO_4^{2-} , and Na^+ , indicating the presence of Ca^{2+} and Mg^{2+} predominantly in the form of chloride and sulphate salts. There was also a strong positive correlation between sodium and chloride. Sodium was generally present in the form of sodium chloride, which was mostly caused by mixing with seawater intrusion. Cu^+ , Pb^{2+} , Cd^{2+} , Mn^{2+} , COD, TOC and BOD all exhibit a significant positive correlation, indicating that these contaminants in water may have common origins such as industrial effluents and municipal wastewater discharge.

Principal component analysis/factor analysis

The influence of sewage treatment plant on groundwater was determined using the same database, which comprised 13 variables. The eigenvalue for each principal component is depicted in the scree plot in Fig. 9. This was utilised to determine which of the principal components should be kept in order to comprehend the basic data structure (Dutta et al. 2018). In the scree plot, there is a noticeable change in slope. Significant principal components are those with eigenvalues greater than unity and the first after unity (Hair et al. 2006).

The factor loadings of the retained principle components are shown in Table 6. Factor loadings are related to the correlation between original variables and principal component loadings in that they aid in understanding the fundamental character of a component (Vega et al. 1998). In various researches, different minimum criteria for factor loadings have been employed to determine which variables are important (Gamble and Babbar-Sebens 2012). Factor loadings greater than 0.5 were deemed to have a significant contribution to the related factor in this investigation. As a

result, factor loads are classified as ‘strong,’ ‘moderate’ and ‘weak,’ with absolute loading values of > 0.75 , $0.75\text{--}0.50$, and $0.50\text{--}0.30$, respectively (Liu et al. 2003).

First, we can see that there are two principal components in the Pleistocene aquifer. Pb^{2+} , Na^+ , Cl^- , Cu^+ , Cd^{2+} , TDS, Mn^+ , BOD, COD, TOC and BOD all contribute significantly to PC1, which explains 57.285% of the variance. In the correlation matrix, these variables were proven to be correlated. PC2 explains 26.199% of the variance and is contributed significantly by PO_4^{3-} , SO_4^{2-} and TH. Second, at the Miocene aquifer, we can observe that there are four principal components. PC1 explains 55.918% of the variance and is contributed significantly by TDS, Cl^- , Na^+ , TH, SO_4^{2-} , Cu^+ , COD and Pb^{2+} . The correlation matrix revealed that these factors were linked. PC2 explains 14.673% of the variance and is contributed significantly by Pb^{2+} and BOD. PC3 explains 9.954% of the variance and includes PO_4^{3-} as the only significant positive loading. Finally, PC4 explains 9.258% of the total variability and is contributed significantly by TOC only. All the principal components have highly random variables, which makes hydrochemical and biological interpretation difficult. As a result, a rotation of the principal components was carried out to get a simpler and relevant portrayal of the underlying factors by increasing the more significant variables. Rotation modifies the variance explained by each factor (Singh et al. 2013). Tables 7, and 8 shows the factor loadings of the varimax rotated components (called varifactors). First, at the Pleistocene aquifer, we can observe that there are two varifactors. Varifactor 1 explains 47.603% of the total variance and is taken part by TDS, Cl^- , Na^+ , COD, Cu^+ , Mn^{2+} , TOC and Pb^{2+} ; this can be interpreted as metal segment and nutrient contamination in the water body. Varifactor 2 explains 35.881% of the variance and is profoundly contributed by BOD, Cd^{2+} and Pb^{2+} .

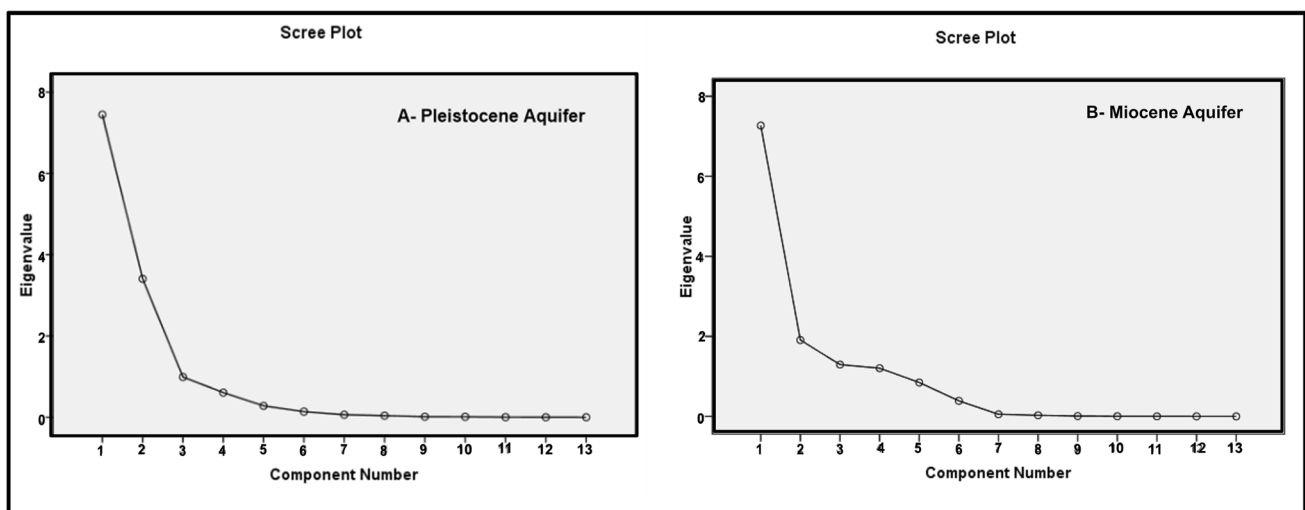


Fig. 9 Scree plots of Pleistocene and Miocene aquifer

Table 6 Loadings of the experimental variables on the significant principal components (PCs)

	Component matrix ^a of Pleistocene aquifer			Component matrix ^a of Miocene aquifer			
	PC1	PC2		PC1	PC2	PC3	PC4
Pb ²⁺	0.920	-0.246	TDS	0.992	-0.046	-0.028	-0.084
Na ⁺	0.897	0.416	Cl ⁻	0.992	-0.057	0.000	-0.056
Cl ⁻	0.896	0.435	Na ⁺	0.992	-0.035	-0.004	-0.074
Cu ⁺	0.861	0.293	TH	0.964	-0.160	-0.118	-0.027
PO ₄ ³⁻	-0.844	0.502	SO ₄ ²⁻	0.956	-0.051	-0.168	-0.194
Cd ²⁺	0.816	-0.431	Cu ⁺	0.920	0.210	-0.087	-0.248
TDS	0.794	0.597	COD	0.874	-0.300	0.146	0.326
Mn ²⁺	0.758	0.120	Pb ²⁺	0.730	0.664	0.010	0.020
COD	0.741	0.475	BOD	0.100	0.834	0.120	0.402
TOC	0.569	0.160	Mn ²⁺	0.352	-0.691	-0.0108	0.547
SO ₄ ²⁻	-0.175	0.930	TOC	0.161	-0.112	0.0703	-0.521
BOD	0.555	-0.699	Cd ²⁺	0.089	0.274	-0.637	0.003
TH	-0.676	0.696	PO ₄ ³⁻	0.404	0.193	0.544	0.500
% of Variance	57.285	26.199	% of Variance	55.918	14.673	9.954	9.258
%Cumulative	57.285	83.484	%Cumulative	55.918	70.591	80.545	89.803

It can be defined as heavy metal and biological pollution of a water body as a result of industrial and municipal wastewater discharges. These heavy metals are substantially associated with each other, as seen in the correlation table. Second, at the Miocene aquifer, we can observe that there are four varifactors. Varifactor 1 explains 52.398% of the variance and is taken part by SO₄²⁻, TDS, Na⁺, Cl⁻, Cu⁺, TH, COD and Pb²⁺. Varifactor 2 explains 13.716% of the variance and is chiefly contributed by TH, BOD and PO₄³⁻. Varifactor 3 explains 13.403% of the variance and includes TOC and SO₄²⁻. Finally, varifactor 4 explains 10.286% of the total

variability and is contributed significantly by TOC only. Organic contamination, which results from the regular flow of residential wastewater into groundwater, is represented by varifactors 3 and 4.

The study used the Kaiser–Meyer–Olkin (KMO) and Bartlett tests of sphericity to ensure that the dataset was suitable for principal component analysis (PCA) and factor analysis (FA). KMO is a sampling adequacy calculation that indicates the amount of variance produced by underlying principal components (PCs) (Mitra et al. 2018). Generally, KMO values below 0.5 are undesirable, whereas values ranging from 0.5 to

Table 7 Loadings of the experimental variables on the rotated significant principal components

Rotated component matrix ^a of Pleistocene aquifer	Rotated component matrix ^a of Pleistocene aquifer		Rotated component matrix ^a of Miocene aquifer	Rotated component matrix ^a of Miocene aquifer			
	Varifactor 1	Varifactor 2		Varifactor 1	Varifactor 2	Varifactor 3	Varifactor 4
TDS	0.992	-0.052	SO ₄ ²⁻	0.986	-0.029	0.077	-0.055
Cl ⁻	0.986	0.139	TDS	0.978	0.095	0.165	0.045
Na ⁺	0.976	0.156	Na ⁺	0.973	0.118	0.165	0.061
COD	0.881	0.019	Cl ⁻	0.968	0.114	0.192	0.065
Cu ⁺	0.878	0.237	Cu ⁺	0.958	0.148	-0.138	-0.035
Mn ²⁺	0.696	0.323	TH	0.945	0.010	0.273	-0.025
TOC	0.562	0.185	COD	0.740	0.191	0.610	0.156
TH	-0.173	-0.954	Pb ²⁺	0.700	0.622	-0.276	-0.144
BOD	0.071	0.890	BOD	-0.013	0.884	-0.230	-0.214
PO ₄ ³⁻	-0.420	-0.888	PO ₄ ³⁻	0.204	0.698	0.330	0.331
SO ₄	0.374	-0.869	Mn ²⁺	0.209	-0.149	0.919	-0.055
Cd ²⁺	0.437	0.813	TOC	0.208	-0.093	-0.259	0.828
Pb ²⁺	0.626	0.717	Cd ²⁺	0.156	-0.019	-0.173	-0.658
% of Variance	47.603	35.881	% of Variance	52.398	13.716	13.403	10.286
%Cumulative	47.603	83.484	%Cumulative	52.398	66.114	79.517	89.803

Table 8 The overall quality (Ow) of the groundwater samples

No	OW pH	OW Na ⁺	OW K ⁺	OW Ca ²⁺	OW Mg ²⁺	Ow Cl ⁻	OW HCO ₃ ⁻	OW SO ₄ ²⁻	OW NO ₃ ⁻	OW Cd ²⁺	OW Cu ⁺	OW Mn ²⁺	OW Pb ²⁺	ΣOW
G2	0.059	0.673	0.088	0.152	0.142	0.807	0.053	0.540	0.007	6.475	3.132	0.254	0.46	12.8
G4	0.059	0.731	0.091	0.344	0.200	0.949	0.037	1.020	0.011	0.151	0.073	0.008	0.08	3.8
G5	0.063	0.731	0.160	0.097	0.156	0.949	0.037	0.308	0.005	0.195	0.094	0.012	0.15	3.0
G6	0.066	0.558	0.083	0.111	0.127	0.743	0.038	0.250	0.005	1.730	0.837	0.027	1.52	6.1
G8	0.065	0.884	0.114	0.113	0.154	1.218	0.041	0.185	0.013	0.847	0.410	0.015	0.83	4.9
G9	0.065	0.654	0.112	0.084	0.158	0.680	0.041	0.577	0.002	2.456	1.188	0.034	2.94	9.0
G11	0.059	0.904	0.086	0.132	0.153	1.155	0.044	0.346	0.017	0.003	0.001	0.186	0.16	3.2
G13	0.062	0.980	0.128	0.126	0.198	1.329	0.038	0.280	0.016	1.294	0.626	0.056	0.86	6.0
G14	0.063	1.019	0.160	0.096	0.156	1.297	0.035	0.317	0.008	1.285	0.621	0.034	0.08	5.2
G15	0.061	1.000	0.106	0.180	0.179	1.518	0.034	0.281	0.008	0.068	0.033	0.006	0.08	3.6
G16	0.067	0.769	0.088	0.067	0.117	0.996	0.041	0.182	0.002	0.059	0.028	0.067	0.08	2.6
G17	0.060	0.634	0.088	0.129	0.132	0.981	0.037	0.133	0.023	3.214	1.555	0.149	0.08	7.2
G18	0.063	0.961	0.112	0.257	0.208	1.550	0.031	0.385	0.006	0.324	0.157	0.006	0.73	4.8
G19	0.065	1.057	0.160	0.178	0.186	1.582	0.023	0.327	0.007	0.151	0.073	0.186	1.58	5.6
G21	0.060	0.807	0.106	0.162	0.172	1.170	0.032	0.374	0.003	8.636	4.178	0.045	1.96	17.7
G22	0.063	1.346	0.160	0.258	0.206	1.866	0.037	0.466	0.002	7.916	3.829	0.263	0.08	16.5
G23	0.060	1.038	0.122	0.338	0.169	1.423	0.021	0.827	0.003	0.064	0.031	0.006	0.75	4.9
G24	0.060	0.827	0.104	0.394	0.186	1.297	0.013	0.750	0.003	1.767	0.855	0.027	0.27	6.5
G1	0.059	0.223	0.080	0.157	0.126	0.293	0.038	0.516	0.018	24.18	11.69	19.04	1.28	57.7
G3	0.061	0.446	0.072	0.072	0.087	0.569	0.039	0.177	0.005	2.850	1.379	21.01	0.08	26.9
G7	0.063	0.231	0.051	0.066	0.090	0.387	0.034	0.054	0.002	2.581	1.249	23.02	0.08	27.9
G25	0.062	0.500	0.066	0.068	0.096	0.633	0.055	0.177	0.005	0.140	0.068	10.19	0.08	12.1
G26	0.059	0.223	0.058	0.105	0.096	0.419	0.069	0.061	0.014	0.554	0.268	14.73	0.96	17.6
G27	0.060	0.531	0.067	0.097	0.096	0.664	0.051	0.279	0.005	0.178	0.086	19.36	1.01	22.5
G29	0.061	0.446	0.088	0.098	0.116	0.696	0.042	0.181	0.007	0.320	0.155	19.04	1.13	22.4

0.7 are considered sufficient and higher values (above 0.7) are exceptionally good (Ustaoğlu et al. 2020). The current study achieved KMO value of 0.577 and 0.444 for Pleistocene and Miocene aquifers, respectively. Bartlett's test examines the possibility of the correlation matrix being an identity matrix. If such a possibility exists, Bartlett's test of sphericity assumes that all variables are unrelated and dimensionality reduction is not feasible, thus making PCA and FA inapplicable. Bartlett's test values of less than 0.050 are favourable, indicating that there are substantial correlations between variables (Tripathi and Singal 2019). In the current case, Bartlett's significance level is 0.000 for both aquifers, thus confirming the appropriateness to perform principal component analysis and factor analysis (Banda and Kumarasamy 2020).

Cluster analysis

Based on the database of 13 variables that include TDS, TH, Cl^- , SO_4^{2-} , Na^+ , PO_4^{3-} , BOD, TOC, COD, Cd^{2+} , Cu^+ , Pb^{2+} and Mn^{2+} , the water samples were grouped into clusters according to similarities. The hierarchical clustering analysis (HCA) was carried out using surface water and groundwater samples (Pleistocene and Miocene) from several classes, based on similarities within a class and dissimilarities between different classes. The results of HCA showed that 31 water points in the Pleistocene, the Miocene and the surface water, respectively, were classified into four types of cluster groups (Fig. 8a–d) according to observations and variables. In the dendrogram (Fig. 8a) according to observations, three distinct clusters (C1, C2 and C3) are formed. G2, G9, G5, G16, G17, G6, treatment plant 2 and S10 form the first cluster (C1). The second cluster (C2) consists of G4, G23, G24, G8, G11, G21, G13, G14, G15, G19, G18, S28, S22 and treatment plant 1. These two clusters show low levels of heavy metal pollution and moderate levels of faecal and organic pollution, and the third cluster (C3) consists of two surface water S12 and S20; this cluster shows high level of heavy metals and faecal contamination. As shown in Fig. 8b, two distinct clusters are formed according to variables. C1 and C2 comprised the upstream section and downstream of the study area that received wastewater from water treatment plant. Therefore, the influence of surface water and treatment plant on groundwater is identified. In the dendrogram in Fig. 8c, also three distinct clusters are formed according to observations. The first cluster consists of G1, G7, G26, S10, G3, G27, G29, G25 and treatment plant 2; this cluster shows low level of pollution. The second cluster (C2) consists of S25 and treatment plant 1; this cluster shows high level of pollution. The third cluster (C3) consists of S12 and S20, and this cluster shows moderate level of pollution. The first cluster shows treatment plant effects on groundwater. In the dendrogram in Fig. 8d, four distinct clusters are formed according to variables. These clusters (C1, C2) show high level of heavy metals and faecal

contamination in the dendrogram. HCA showed that the possible pollution sources for the most polluted water sources were natural sources such as water treatment plant and surface runoff, with high contributions of PO_4^{3-} , BOD, TOC, COD, Cd^{2+} , Cu^+ , Pb^{2+} and Mn^{2+} , outside of WHO norms.

Pollution indices

Heavy metal pollution index

The concentrations of heavy metals in groundwater such as Fe^{2+} , Mn^{2+} , Pb^{2+} , Cu^+ , Cd^{2+} , Ni^{2+} , Cr^{3+} , Co^{2+} , Mo^{2+} , V^{5+} and Zn^{2+} are listed in Table 5. From the results, it has been observed that concentrations of heavy metals such as Fe^{2+} , Ni^{2+} , Cr^{3+} , Co^{2+} , Mo^{2+} , V^{5+} and Zn^{2+} were well below the permitted limits established by WHO (2017) for drinking water. The concentration of Mn^{2+} , Cd^{2+} , Cu^+ and Pb^{2+} has been found to be more than the desirable limit of drinking water standard at many places, in both aquifers. The mean concentrations were calculated to guess the heavy metal pollution index (Panigrahy et al. 2015). Calculated index values and unit weightage values are listed in Table 1. The HPI for the study area is intended by integrating the mean concentration values of confirmed heavy metals. The particulars of the calculation are shown in Table 2B. HPI is categorised into five classes: excellent (0–25), good (26–50), poor (51–75), very poor (76–100) and unsuitable (100). Moreover, 77% of the Pleistocene aquifer samples is considered unsuitable for drinking purposes, 6% very poor and the remaining samples (17%) is considered good; on the other hand, 72% of the Miocene aquifer samples is considered unsuitable for drinking purposes, and the remaining 28% is considered good. The results were assessed that in both aquifers (Pleistocene, Miocene), the heavy metal pollution index exceeds 100 in the majority of the samples. Wells are shown to be contaminated by heavy metals. It was estimated that the region of the research would be affected by heavy metal leakage from the water treatment plant, as shown in Fig. 3b. The water treatment plant has not treated the inorganic matters especially the heavy metals.

Nitrate pollution index

Nitrate levels were ranged from 1 to 13.2 mg/l with an average of 4.03 mg/l in the study area. Nitrate was organized into three groups: (1) low (< 20 mg/l), (2) medium (≥ 20 to < 50 mg/l) and (3) high (≥ 50 mg/l). The concentration of nitrate in all the samples in the studied area is less than 20 mg/l. Five classifications of water have been determined according to NPI values: clean, light pollution, moderate pollution, significant pollution and highly significant pollution, with NPI values of < 0, 0–1, 1–2,

2–3 and > 3, respectively. NPI is smaller than zero for all groundwater samples in the class clean (Table 10).

Pollution index of groundwater

The relative contribution of the pollutants from each ground water sample was evaluated in a Pollution Index (PIG) assessment. The chemical water quality (Ow) of pH and NO3 of less than 0.1 (Table 8) shows a low impact on groundwater contamination in the current study. Based on the data in Table 8, Na+, Cl-, Ca2+, Mg2+, SO42-, Cd2+, Cu+, Mn2+ and Pb2+ had the most significant on sample water quality. This is evident in the values of Ow and PIG achieved. In the present study, the final PIG values were around 2.6 and 57.7. In five categories, the level of drinking water pollution is divided: PIG < 1.0 indicates insignificant pollution; 1.0–1.5 refers to the low pollution; 1.5–2.0 is moderate pollution; 2.0–2.5 signifies high pollution; PIG > 2.5 shows very high pollution (Table 9) (Rao 2012; Rao et al. 2018; Rao and Chaudhary 2019). Based on this classification, all groundwater samples were found to be very high polluted and therefore are very unsuitable for drinking purposes. Unfit-to-drink samples are detected in both the north and south of the research area, which indicates a substantial anthropogenic influence on the water supply (Fig. 3c)

Ecological risk index

For each heavy metal in Cd2+, Cu+, Mn2+ and Pb2+ and water sample, the RI (potential ecological risk) was initially identified during the ERI evaluation (Table 9). According to Bhutiani et al. (2017), Adimalla and Wang (2018) and Taiwo et al. (2019), RI is divided into five, to reflect its impact on sample quality of heavy metal: RI < 40 (low potential risk), 40 ≤ RI < 80 (moderate potential risk), 80 ≤ RI < 160 (considerable potential risk), 160 ≤ RI < 320 (high potential risk) and ≥ 320 (very high potential risk). In the current study, depending on the classification, Cu+ and Mn+ pose low potential ecological risk. However, it was observed that Cd2+ poses high potential ecological risk to samples G2, G9, G16,

G19, G21, G7, G26 and G27 while Pb2+ poses moderate ecological risk to sample G6, G8, G13, G19, G23, G1, G26, G27 and G29. Table 10 depicts the ecological risk (Er) due to individual metals and ERI by location, while Fig. 3d shows spatial variation of ecological risk due to heavy metals in the study area. The final ERI values achieved from this analysis ranged from 10.9 to 387.5 (Table 10). The ground water can be divided into four categories based on the ERI values: ERI < 150 (low ecological risk), 150 < ERI < 300 (moderate ecological risk), 300 < ERI < 600 (considerable ecological risk) and > 600 (very high ecological risk) (Adimalla and Wang 2018; Taiwo et al. 2019). According to this classification scheme (Table 9), 66.7% of the Pleistocene aquifer samples have low ecological risk, 22.2% have moderate risk and 11% are considerable risks. However, 42.8% of the Miocene aquifer have low ecological risk, 42.8% have moderate risk and 14.4% are a considerable risk.

Irrigation water qualities

The physical and chemical qualities of water, especially dissolved salts, determine its suitability for irrigation. Water evaporates normally, leaving the dissolved salts in the soil complex. The gradual deposit of salt in the soil increases after a few years (Srinivasamoorthy et al. 2014), resulting in a toxicity and salinity hazard. Indices that assist in determining the suitability of irrigation water is explained in the following parts accordingly.

Sodium percentage (Na %)

All concentrations are given in milliequivalents per litre (meq/l) (Table 11). Water is categorised as safe or harmful based on its salt content. For agricultural activities, a Na% of greater than 60 is regarded dangerous, whereas a Na% of less than 60 is considered safe (Eaton 1950; Ravikumar et al. 2011). The Na% the study area is given in Table 9. Moreover, 88.2% of groundwater in Pleistocene aquifer was doubtful and 11.8 was unsuitable, while in Miocene aquifer 28.6% groundwater was permissible and 71.4% was doubtful. EC

Table 9 Groundwater classification based on the PIG and ERI

Quality index	Range of values	Classification
PIG (Subba Rao et al. 2018)	< 1.0	Insignificant pollution
	1.0–1.5	Low pollution
	1.5–2.0	Moderate pollution
	2.0–2.5	High pollution
	> 2.5	Very high pollution
ERI (Bhutiani et al. 2017; Taiwo et al. 2019)	< 150	Low ecological risk
	150 < ERI < 300	Moderate ecological risk
	300 < ERI < 600	Considerable ecological risk
	> 600	Very high ecological risk

Table 10 The potential ecological risks (RI) and heavy metal pollution index (HPI) of the groundwater samples

Sample	RI (Cd ²⁺)	RI (Cu ⁺)	RI (Mn ²⁺)	RI (Pb ²⁺)	∑RI	HPI	NPI	Na ⁺ %	SAR
Pleistocene aquifer									
G2	191	6.32	0.34	24.10	224.6	221.8	−0.705	72	20
G4	6	0.15	0.01	4.00	10.9	10.2	−0.86	61	16
G5	6	0.19	0.02	7.65	24.1	13.9	−0.875	77	23
G6	6	1.69	0.04	78.95	88.0	86.7	−0.67	73	18
G8	6	0.83	0.02	42.90	50.7	49.7	−0.95	79	27
G9	204	2.40	0.05	152.65	360.6	359.1	−0.565	75	21
G11	134	0.00	0.01	8.40	143.1	142.4	−0.595	78	27
G13	119	1.26	0.08	44.45	166.0	164.8	−0.78	77	27
G14	72	1.25	0.05	4.00	78.4	77.3	−0.79	82	32
G15	83	0.07	0.01	4.00	87.8	87.1	−0.95	76	26
G16	212	0.06	0.01	4.00	224.1	216.1	−0.39	82	28
G17	6	3.14	0.20	4.00	21.3	13.3	−0.84	73	20
G18	6	0.32	0.00	38.20	47.6	44.5	−0.825	70	22
G19	270	0.15	0.01	82.10	353.0	352.3	−0.925	77	28
G21	171	8.42	0.06	101.70	285.2	281.2	−0.95	73	22
G22	6	7.72	0.35	4.00	23.0	18.1	−0.93	77	31
G23	9	0.06	0.01	39.00	63.0	48.1	−0.92	70	23
G24	6	1.72	0.04	13.90	25.4	21.7	−0.54	62	17
Miocene aquifer									
G1	6	23.59	0.64	66.40	106.5	96.6	−0.865	48	7
G3	6	2.78	0.09	4.00	14.5	12.9	−0.645	76	18
G7	247	2.52	0.10	4.00	261.5	253.6	−0.86	63	9
G25	6	0.14	0.03	4.00	12.0	10.2	−0.81	77	19
G26	172	0.54	0.01	49.95	223.7	222.5	NPI	56	8
G27	335	0.17	0.02	52.30	388.3	387.5	−0.815	76	19
G29	154	0.31	0.02	58.55	213.7	212.9	−0.705	70	15

Table 11 Suitability for irrigation based on sodium percent (Na%)

Na%	Suitability for irrigation	The percentages of the Pleistocene aquifer	The percentages of the Miocene aquifer
<20	Excellent	–	–
20–40	Good	–	–
40–60	Permissible	–	28.6
60–80	Doubtful	88.2	71.4
>80	Unsuitable	11.8	–

and Na% are plotted in Fig. 10 which showed that most of the groundwater samples were doubtful for agriculture. Irrigation water is classified according to its soluble sodium level because irrigation water with higher sodium content has lower permeability. Increased sodium and salinity hazards cause the quality of irrigation water to deteriorate.

Sodium adsorption ratio (SAR)

High SAR values (Table 10) indicate a tendency for water to replace adsorbed Ca²⁺ and Mg²⁺ with salt, affecting irrigation quality and harming soil structure. This will also lead to a decrease in infiltration and permeability of the soil to water leading to problems with crop production. According to the U.S. salinity classification (Table 12), the water is divided into four classes on the basis of salinity (C1, C2, C3 and C4) and four classes on the basis of SAR (S1, S2, S3 and S4) (Richards 1954). Groundwater samples of the Pleistocene aquifer in the study area lie in the fields C4-S2 (17.6%), C4-S3 (41.2%) and C4-S4 (41.2%), while in Miocene aquifer groundwater samples lie in the fields C4-S1 (42.8%), C4-S2 (28.6%) and C4-S3 (28.6%). Both groundwater samples are not suitable for irrigation under ordinary conditions, but may be used occasionally under special conditions as the soils must be permeable. The use of such water for irrigation may damage the soil structure, which in turn affects the water infiltration capacity and permeability of soil (Prasanth et al. 2012).

Fig. 10 Suitability of ground-water for irrigation purpose based on sodium percentage (%)

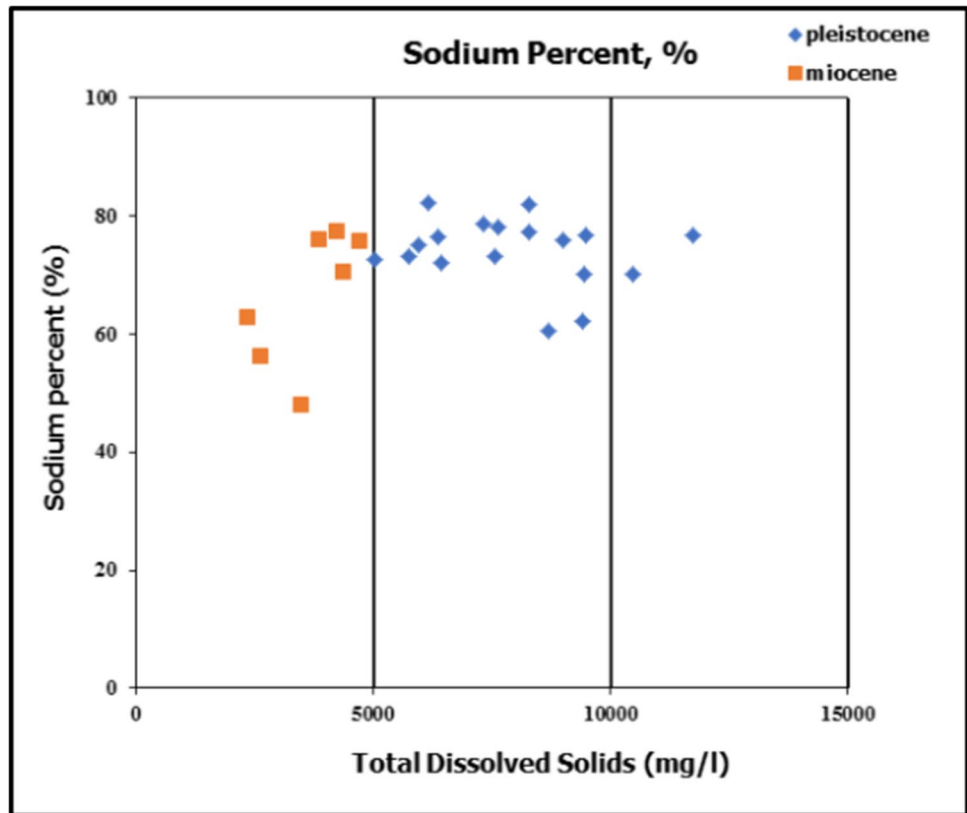


Table 12 The water quality classes according to the U.S. Salinity Laboratory Staff, (Richards, 1954)

EC	Quality	Range
C1	Low salinity water	100–250
C2	Medium salinity water	250–750
C3	High salinity water	750–2250
C4	Very high salinity	>2250
S1	Low sodium water	0–10
S2	Medium sodium water	10–18
S3	High sodium water	18–26
S4	Very high sodium	26–100

Conclusion

In the present study, hydrogeochemical, statistical and pollution index analysis can be employed to better understand the water quality. The influence of surface water on groundwater has been identified. The concentrations of Cl^- and Na^+ in groundwater were higher in study wells due to marine intrusion entering groundwater resources and combining with the marine aquifer matrix. This reflects mixing of groundwater with the matrix of the aquifers which have marine origin. The high salinity values of the groundwater in both aquifers could be attributed

to the geomorphologic and geologic settings of the study area. The values of TDS, Cl^- , SO_4^{2-} , TH and Na^+ were found to be above permissible limits in the groundwater for drinking purposes. This water is unsuitable for human consumption. The data of Na^+ , Cl^- , Ca^{2+} , Mg^{2+} , SO_4^{2-} , Cd^{2+} , Cu^+ , Mn^{2+} and Pb^{2+} had the most significant effect on sample water quality. In the present study, the final pollution indexes of groundwater (PIG) values were around 2.6 and 57.7. All groundwater samples were very highly polluted and unfit for human use. Multivariate statistics were successfully applied to evaluate the variation in the water quality of groundwater and to identify the factors responsible for the pollution in the study area. Principal component analysis (PCA) identified several variables and varifactors, giving forward a hydrochemical meaning. First, at the Pleistocene aquifer, minerals and nutrient pollution were identified for varifactor 1, and heavy metal and biological pollution for varifactor 2. Second, at the Miocene aquifer, minerals and nutrient pollution were identified for varifactor 1, and biological pollution for varifactor 2. Organic contamination, which results from the regular flow of residential wastewater into groundwater, is represented by varifactors 3 and 4. To determine the impact of surface water and treatment plant on groundwater, water samples were classified into clusters. Water quality in the research area is influenced by both natural and man-made environmental factors. The HCA found three water

pollution clusters: low, moderate and high. HCA revealed that natural sources such as water treatment plants and surface runoff were likely contamination sources for the most polluted water sources. Ecological risk index (ERI) of most groundwater samples showed moderate ecological risk due to metal contamination. Regarding sodium percent (Na%) and sodium adsorption ratio (SAR), the groundwater is unsuitable for irrigation purposes.

Recommendations (suggested solutions)

This research recommends the treatment of contaminated groundwater before human consumption. In addition, groundwater protection strategies should be implemented because the aquifers are rather shallow. Chemical analyses must be carried out periodically for groundwater to determine any water quality changes. Monitoring of the seepage of groundwater from the contaminant drains in such area will be necessary, as well as the development of a treatment plant that includes the inclusion of a triple-stage filtration and disinfection process, which includes the use of chlorine gas for sanitation before and after filtration to assure the elimination of all viruses, bacteria, and worms, and that the water must meet the standard set by the Ministry of Health.

Author contribution All authors contributed to the study conception and design. Material preparation, data collection and analysis were performed by RAE, EZ, HI, EAS, MMHK, AME and MMS. The first draft of the manuscript was written by RAE and all authors commented on previous versions of the manuscript. All authors read and approved the final manuscript.

Funding The authors declare that they have no known competing financial interests or personal relationships that could have appeared to influence the work reported in this paper. No funding source(s) for this research has been received.

Data availability The datasets used and/or analysed during the current study are available from the corresponding author on reasonable request.

Declarations

Competing interests The authors declare no competing interests.

References

Adimalla N, Wang H (2018) Distribution, contamination, and health risk assessment of heavy metals in surface soils from northern Telangana. *India Arab J Geosci* 11(21):1–15

Adimalla N, Wu J (2019) Groundwater quality and associated health risks in a semi-arid region of south India: implication to

sustainable groundwater management. *Hum Ecol Risk Assess Int J* 25(1–2):191–216

Alexakis D (2011) Assessment of water quality in the Messolonghi-Etoliko and Neochorio region (West Greece) using hydrochemical and statistical analysis methods. *Environ Monit Assess* 182(1):397–413

Ali, A., Oweis, T., Rashid, M., El-Naggar, S., & Aal, A. A. (2007). Water harvesting options in the drylands at different spatial scales. *Land Use and Water Resources Research*, 7(1732–2016–140274)]

Al-Sayed E., El-Qady G., El-Kenawy A., (2016). Ground water exploration and mapping the seawater intrusion at Matruh area, North Coast, Egypt. Conference: The 7th International Conference on Water Resources and Arid Environments (2016) At: Saudi Arabia.

American Society for Testing and Materials [ASTM], (2002). Water and Environmental Technology, Annual Book of ASTM Standards, U.S.A. Sect.11.Vols.11.01, And 11.02, Conshohocken.

Banda TD, Kumarasamy M (2020) Application of multivariate statistical analysis in the development of a surrogate water quality index (WQI) for South African watersheds. *Water* 12(6):1584

Barseem, M. S. (2006). *Geophysical contribution to groundwater exploration in carbonate rocks, West Sidi Barani area, northwestern coast, Egypt* (Doctoral dissertation, Ph. D. Thesis, Faculty of Science, Menoufia University)]

Barseem M, El Tamamy AM, Masoud M (2013) Hydrogeophysical evaluation of water occurrences in El Negila area, Northwestern coastal zone–Egypt. *J Appl Sci Res* 9(4):3244–3262

Bhutiani R, Kulkarni DB, Khanna DR, Gautam A (2017) Geochemical distribution and environmental risk assessment of heavy metals in groundwater of an industrial area and its surroundings, Haridwar, India. *Energy Ecol Environ* 2(2):155–167

Bora M, Goswami DC (2017) Water quality assessment in terms of water quality index (WQI): case study of the Kolong River, Assam. *India Appl Water Sci* 7(6):3125–3135

Brindha K, Vaman KN, Srinivasan K, Babu MS, Elango L (2014) Identification of surface water-groundwater interaction by hydro-geochemical indicators and assessing its suitability for drinking and irrigation purposes in Chennai. *South India Appl Water Sci* 4(2):159–174

Brown, R. M., McClelland, N. I., Deininger, R. A., & Tozer, R. G. (1970). A water quality index—do we dare. *Water and sewage works*, 117(10)]

Butzer, K. W. (1959). Environment and human ecology in Egypt during predynastic and early dynastic times. Reprinted from *Bulletin de la Société de Géographie d’Égypte*, t. 32]

CLAC, (2015). Central Laboratory for Agricultural Climate website. <http://www.calc.edu.eg>.

Dutta S, Dwivedi A, Kumar MS (2018) Use of water quality index and multivariate statistical techniques for the assessment of spatial variations in water quality of a small river. *Environ Monit Assess* 190(12):1–17

Eaton FM (1950) Significance of carbonates in irrigation waters. *Soil Sci* 69(2):123–134

Edokpayi, J. N., Odiyo, J. O., & Durowoju, O. S. (2017). Impact of wastewater on surface water quality in developing countries: a case study of South Africa. *Water quality*, 401–416]

Eissaa M. A., de Dreuzy Jean-R., B. Parker (2018). Integrative management of saltwater intrusion in poorly-constrained semiarid coastal aquifer at Ras El-Hekma, Northwestern Coast, Egypt. *Groundwater for Sustainable Development*, Volume 6, March 2018, Pages 57–70.

El Bastawesy, M. A., NASR, A., & Ali, R. R. (2008). The use of remote sensing and GIS for catchment delineation in northwestern coast of Egypt: an assessment of water resources and soil potential. *Egyptian Journal of Remote Sensing and Space Sciences*, 11]

El Shazly, M. M. (1964). Geology, pedology and hydrogeology of Mersa Matruh area, Western Mediterranean littoral. PhD Thesis, Cairo University, Cairo, Egypt.

- Fishman, M. J., & Friedman, L. C. (1989). *Methods for determination of inorganic substances in water and fluvial sediments*. US Department of the Interior, Geological Survey.]
- Gamble A, Babbar-Sebens M (2012) On the use of multivariate statistical methods for combining in-stream monitoring data and spatial analysis to characterize water quality conditions in the White River Basin, Indiana, USA. *Environ Monit Assess* 184(2):845–875
- Gamvroula D, Alexakis D, Stamatis G (2013) Diagnosis of groundwater quality and assessment of contamination sources in the Megara basin (Attica, Greece). *Arab J Geosci* 6(7):2367–2381
- Giménez-Forcada E (2010) Dynamic of sea water interface using hydrochemical facies evolution diagram. *Groundwater* 48(2):212–216
- Guesdon G, Santiago-Martín D, Raymond S, Messaoud H, Michaux A, Roy S, Galvez R (2016) Impacts of salinity on Saint-Augustin Lake, Canada: Remediation measures at watershed scale. *Water* 8(7):285
- Hair JE, William CB, Barry JB, Rolph EA, Tatham RL (2006) *Multivariate data analysis*, 6th edn. Pearson Prentice Hall, New Jersey
- Hammad FA (1966) The geology of water supplies in Ras El Hekma area. Thesis, Cairo University, Cairo, Egypt, M.Sc
- Hammad, F. A. (1972). The geology of soils and water resources in the area between Ras El Hekma and Ras El Rum (Western Mediterranean Littoral Zone, Egypt). Ph.D. Dissertation, Fac. Sci., Cairo University.
- Horton RK (1965) An index number system for rating water quality. *J Water Pollut Control Fed* 37(3):300–306
- Kaiser HF (1974) An index of factorial simplicity. *Psychometrika* 39(1):31–36
- Khatri N, Tyagi S (2015) Influences of natural and anthropogenic factors on surface and groundwater quality in rural and urban areas. *Frontiers in Life Science* 8(1):23–39
- Liu, C. W., Lin, K. H., & Kuo, Y. M. (2003). Application of factor analysis in the assessment of groundwater quality in a blackfoot disease area in Taiwan. *Science of the total environment*, 313(1–3), 77–89. London.
- Manahan SE (2010) *Water chemistry: green science and technology of nature's most renewable resource*. CRC Press
- Masoud MHZ (2000) Assessment of surface runoff in Marsa Matrouh area, Northwestern Coastal Zone, Egypt (Doctoral dissertation. Thesis, Faculty of Science, Alexandria University, Egypt), M.Sc
- Matiatos I, Alexopoulos A, Godelitsas A (2014) Multivariate statistical analysis of the hydrogeochemical and isotopic composition of the groundwater resources in northeastern Peloponnesus (Greece). *Sci Total Environ* 476:577–590
- McLay CDA, Dragten R, Sparling G, Selvarajah N (2001) Predicting groundwater nitrate concentrations in a region of mixed agricultural land use: a comparison of three approaches. *Environ Pollut* 115(2):191–204
- Mitra S, Ghosh S, Satpathy KK, Bhattacharya BD, Sarkar SK, Mishra P, Raja P (2018) Water quality assessment of the ecologically stressed Hooghly River Estuary, India: a multivariate approach. *Mar Pollut Bull* 126:592–599
- Mohamed A, El Sabri SH, Masoud MHZ, Kamal Dahab A (2011) Water budget assessment for some wadis west Marsa Matruh and possibilities of sea water intrusion. *Sedimentology of Egypt* 1:113–125
- Mohamed I, Othman F, Ibrahim AIN, Alaa-Eldin ME, Yunus RM (2015) Assessment of water quality parameters using multivariate analysis for Klang River basin. *Malaysia Environ Monit Assess* 187:4182. <https://doi.org/10.1007/s10661-014-4182-y>
- Mohan SV, Nithila P, Reddy SJ (1996) Estimation of heavy metals in drinking water and development of heavy metal pollution index. *J Environ Sci Health Part A* 31(2):283–289
- Mohankumar K, Hariharan V, Rao NP (2016) Heavy metal contamination in groundwater around industrial estate vs residential areas in Coimbatore India. *J Clin Diagn Res: JCDDR* 10(4):BC05
- Mustafa A, Eissa MA, Mahmoud HH, Shouakar Stash O, El-Shiekh A, Parker B (2016) Geophysical and geochemical studies to delineate seawater intrusion in Bagoush area, Northwestern coast, Egypt. *J African Earth Sci* 121(2016):365e381
- National Authority for Remote Sensing & Space Sciences (NARSS), (2005). Environmental evaluation of land resources in the Northwestern Coast of Egypt, using space data and land information systems, phase II: area from Sedi Abd El-Rahman to Marsa El-Assi. Final Report No. 101/SR/ENV/04–0. Cairo: NARSS.
- Obeidat, M. M., Awawdeh, M., Al-Rub, F. A., & Al-Ajlouni, A. (2012). An innovative nitrate pollution index and multivariate statistical investigations of groundwater chemical quality of Umm Rijam Aquifer (B4), North Yarmouk River Basin, Jordan. *Vouddouris K, Voutsas D. Water Quality Monitoring and Assessment*. Croatia: InTech, 169–188.]
- Otto M (1998) *Multivariate methods*. In: Kellner R, Mermet JM, Otto M, Widmer HM (eds) *Analytical chemistry*. Wiley-VCH, Weinheim, p 916
- Oweis TY, Hachum AY (2003) 11 Improving water productivity in the dry areas of West Asia and North Africa. *Water Product Agric: Limits Oppor Improv* 1:179
- Panigrahy BP, Singh PK, Tiwari AK, Kumar B, Kumar A (2015) Assessment of heavy metal pollution index for groundwater around Jharia coalfield region, India. *J Biodivers Environ Sci* 6(3):33–39
- Piper AM (1944) A graphic procedure in the geochemical interpretation of water-analyses. *EOS Trans Am Geophys Union* 25(6):914–928
- Prasanth SV, Magesh NS, Jitheshlal KV, Chandrasekar N, Gangadhar KJAWS (2012) Evaluation of groundwater quality and its suitability for drinking and agricultural use in the coastal stretch of Alappuzha District, Kerala. *India Applied Water Science* 2(3):165–175
- Ragunath, H. M. (1987). Ground water: hydrogeology, ground water survey and pumping tests, rural water supply and irrigation systems. New Age International.]
- Rainwater, F. H., & Thatcher, L. L. (1960). *Methods for collection and analysis of water samples* (No. 1454–1458). US Government Printing Office.]
- Rao, N. S., & Chaudhary, M. (2019). Hydrogeochemical processes regulating the spatial distribution of groundwater contamination, using pollution index of groundwater (PIG) and hierarchical cluster analysis (HCA): a case study. *Groundwater for Sustainable Development*, 9, 100238.]
- Rao NS, Sunitha B, Adimalla N, Chaudhary M (2020) Quality criteria for groundwater use from a rural part of Wanaparthy District, Telangana State, India, through ionic spatial distribution (ISD), entropy water quality index (EWQI) and principal component analysis (PCA). *Environ Geochem Health* 42(2):579–599
- Rao SN (2012) PIG: a numerical index for dissemination of groundwater contamination zones. *Hydrol Process* 26(22):3344–3350
- Raslan, S. M. (1995). Geomorphological and hydrogeological studies on some localities along the Northwestern Coast of Egypt. *Meno-fia, Egypt*.]
- Ravikumar P, Somashekar RK, Angami M (2011) Hydrochemistry and evaluation of groundwater suitability for irrigation and drinking purposes in the Markandeya River basin, Belgaum District, Karnataka State. *India Environ Monitor Assess* 173(1):459–487
- Richards, L. A. (1954). Diagnosis and improvement of saline and alkali soils. Handbook, 60. USDA, Washington, USA.
- Sewidan, A. S. (1978). *Water budget analysis for the northwestern coastal zone of the Arab Republic of Egypt* (Doctoral dissertation, Ph. D. Thesis, Fac. Sci., Cairo Univ., Egypt).]

- Sherif M, Mahmoudi AE, Garamoon H, Kacimov A, Akram S, Ebraheem A, Shetty A (2006) Geoelectrical and hydrogeochemical studies for delineating seawater intrusion in the outlet of Wadi Ham. *UAE Environmental Geology* 49(4):536–551
- Shrestha S, Kazama F (2007) Assessment of surface water quality using multivariate statistical techniques: a case study of the Fuji river basin. *Japan Environ Model Softw* 22(4):464–475
- Singh EJK, Gupta A, Singh NR (2013) Groundwater quality in Imphal west district, Manipur, India, with multivariate statistical analysis of data. *Environ Sci Pollut Res* 20:2421–2434. <https://doi.org/10.1007/s11356-012-1127-2>
- Smita D, Dwivedi A, Suresh Kumar M (2018) Use of water quality index and multivariate statistical techniques for the assessment of spatial variations in water quality of a small river. *Environ Monit Assess* 190(12):1–17
- Solomon, S., Manning, M., Marquis, M., & Qin, D. (2007). *Climate change 2007—the physical science basis: Working Group I Contribution to the Fourth Assessment Report of the IPCC* (Vol. 4). Cambridge University Press.]
- Srinivasamoorthy K, Gopinath M, Chidambaram S, Vasanthavigar M, Sarma VS (2014) Hydrochemical characterization and quality appraisal of groundwater from Pungar sub basin, Tamilnadu, India *J King Saud University-Sci* 26(1):37–52
- Stiff HA (1951) The interpretation of chemical water analysis by means of patterns. *J Petrol Technol* 3(10):15–23
- Subba Rao N, Sunitha B, Rambabu R, Rao PN, Rao PS, Spandana BD, Marghade D (2018) Quality and degree of pollution of groundwater, using PIG from a rural part of Telangana State, India. *Appl Water Sci* 8(8):1–13
- Taiwo, A. M., Michael, J. O., Gbadebo, A. M., & Oladoyinbo, F. O. (2019). Pollution and health risk assessment of road dust from Osogbo metropolis, Osun state, Southwestern Nigeria. *Human and ecological risk assessment: an international journal*.]
- Tripathi M, Singal SK (2019) Use of principal component analysis for parameter selection for development of a novel water quality index: a case study of river Ganga India. *Ecol Ind* 96:430–436
- Ustaoğlu, F., Tepe, Y., & Taş, B. (2020). Assessment of stream quality and health risk in a subtropical Turkey river system: a combined approach using statistical analysis and water quality index. *Ecological indicators*, 113, 105815.]
- Vega M, Pardo R, Barrado E, Debán L (1998) Assessment of seasonal and polluting effects on the quality of river water by exploratory data analysis. *Water Res* 32(12):3581–3592
- Vijay R, Khobragade P, Mohapatra PK (2011) Assessment of groundwater quality in Puri City, India: an impact of anthropogenic activities. *Environ Monit Assess* 177(1):409–418
- WHO (2017) Guidelines for drinking water quality, 3rd edn. World Health Organization, Geneva
- Wilcox, L. (1955). Classification and use of irrigation waters (No. 969). US Department of Agriculture.]
- Yidana SM, Yidana A (2010) Assessing water quality using water quality index and multivariate analysis. *Environ Earth Sci* 59:1461–1473
- Yousif M (2015) Integration of the geomorphologic and geologic studies for water potentialities development in El Zarraqa and El Harraqa basins, East Matrouh, northwestern coast. *Egypt Arab J Geosci* 8(7):4603–4626
- Yousif M, Oguchi T, Anazawa K, Ohba T (2014) Geospatial information and environmental isotopes for hydrogeological evaluation: Ras Alam El Rum, Northwestern Coast of Egypt. *Nat Resour Res* 23(4):423–445
- Zeuner FE (1959) Jurassic beetles from Grahamland. *Antarctica Palaeontology* 1(4):407–409

Publisher's note Springer Nature remains neutral with regard to jurisdictional claims in published maps and institutional affiliations.